

Carbonaceous Aerosols; a comparison of different Source Regions, Time Intervals and Meteorological Influences in the Netherlands



An artist's impression shows how aerosol particles can serve as seeds for cloud droplets. Credit: NASA;
http://www.nasa.gov/mission_pages/Glory/multimedia/Black_Carbon_Cloud_Droplets.html

Arthur Sebastiaan Kappetijn
Student number: 3407160

Daily Supervisor:
Dr. U. Dusek
Project Supervisor:
Prof. dr. T. Röckmann

Table of Contents

1. Introduction.....	5
1.1 Aerosols.....	5
1.2 Carbonaceous Aerosols.....	7
1.3 Radiocarbon Measurements	9
1.4 “Carbonaceous Aerosols; a comparison of different Source Regions, Time Intervals and Meteorological Influences in the Netherlands”.....	12
2. Methodology	14
2.1 Location.....	14
2.2 High volume Sampler	15
2.3 Filter preparation.....	15
2.4 Thermal Extraction of OC and EC	17
2.5 Meteorological Data.....	21
2.6 Trajectory Model	23
2.7 Overview of collected samples.....	24
2.8 Correction of fraction modern.....	25
3. Results	26
3.1 Fall/winter Samples.....	26
3.2 Day and night filters	35
4. Discussion.....	41
4.1 Fall/winter samples	41
4.2 Day and night samples	44
5. Conclusions.....	48
5.1 Fall/winter samples	48
5.2 Day and night samples	48
6. References	49
7. Appendixes.....	52
Appendix A: THEODORE.....	52

1. Introduction

The main purpose of this thesis is to investigate the influence of weather, source regions and diurnal cycle on the concentration and isotopic composition of organic and elemental carbon on a rural site in the Netherlands.

In this introduction the different terms and definitions will be clarified, followed by the thesis objectives.

1.1 Aerosols

An aerosol is usually defined as solid particles, with particle diameters ranging from 10^{-9} to 10^{-4} meter, “floating” in a gas. Clouds as such fall into this definition with particle diameters of approximately $10\ \mu\text{m}$ but it mainly contains condensed water vapor and clouds are therefore considered as separate phenomena in atmospheric science.

It is important to realize that concentration, composition and size distribution of atmospheric aerosol particles are temporally and spatially highly variable. In the troposphere the total particle number and mass concentrations typically vary in the range of about 10^2 – $10^5\ \text{cm}^{-3}$ and 1 – $100\ \mu\text{g m}^{-3}$, respectively. The Netherlands are considered one of the hotspot areas in Europe with high concentrations of particulate matter (Mooibroek et al., 2011).

There are many ways to characterize aerosols;

- Primary versus secondary aerosols.

Primary aerosols are directly emitted into the atmosphere as liquids or solids from a wide variety of anthropogenic or natural sources. For example biomass burning, (incomplete) combustion of fossil fuels, wind-driven or traffic-related suspension of road, soil, and mineral dust, sea salt, volcanic eruptions and biological materials (plant fragments, microorganisms, pollen, etc.)

Secondary aerosols are created in the atmosphere through several different chemical reactions. A gas to particle conversion occurs for example with sulfuric acid (H_2SO_4) produced by oxidation of natural dimethyl sulfide (DMS) emitted from the ocean surface.

- Natural versus anthropogenic sources.

Anthropogenic aerosols are produced by humans for example fossil fuel burning, biomass burning, agriculture and livestock creates sulfate, ammonium, nitrate, organics and soot. Natural aerosols have different sources such as mineral dust blown in the air by the wind, sea salt from waves, plant fragments, microorganisms, volcanic SO_2 , pollen and wild fires.

- Marine versus continental sources.

Both sources have their specific composition. Marine sources are less polluted containing sea salt and DMS from sulfate.

- Size distribution.

There are three lognormal modes in which aerosols can be divided; the nucleation or ultrafine mode, the accumulation mode and the coarse mode. These are illustrated in figure 1.1.

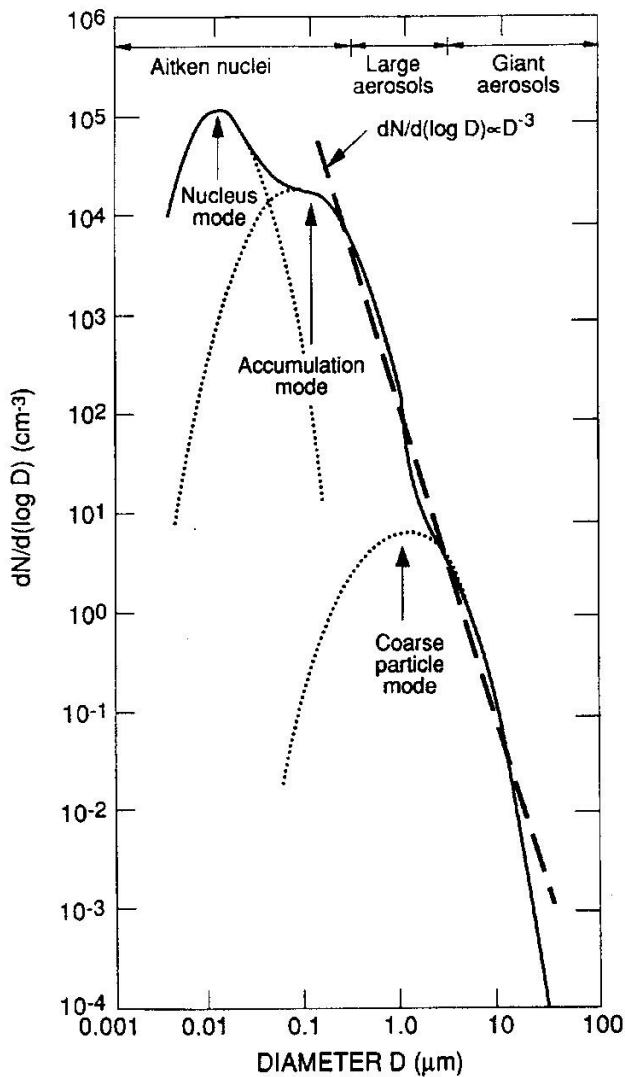


Figure 1.1, size distribution of aerosol; nucleus mode, accumulation mode and coarse mode. Picture from “Atmospheric Composition and Chemical Processes, Aerosol clouds and radiation”, by G.J. Roelofs, 2010.

Once in the atmosphere, three processes can remove tropospheric aerosol particles. Transport to the stratosphere, wet deposition by precipitation and dry deposition. In general stratospheric transport is not a very important removal system. Dry deposition mainly occurs due to gravitational settling or by Brownian diffusion. The fall velocity, or settling velocity, of aerosols depends on their size, shape and weight. Gravitational force is less important than Brownian diffusion for particles smaller than 0,1 micrometer. In that case rapidly moving air molecules collide with small aerosols influencing their motions. This Brownian diffusivity is inversely proportional with the size of these particles.

The residence time of aerosols in the atmosphere strongly depends on their size. Particles in the coarse mode are efficiently removed from the troposphere by the gravitational force of the Earth. Particles in the fine mode are strongly influenced by Brownian diffusion. But aerosols in the accumulation mode are too big for Brownian diffusion and too small to be influenced by gravitational force. These “accumulation”

particles have a residence time of approximately a week, while aerosols in the other modes are effectively removed within a few hours or days. Particles in the accumulation mode can either serve as cloud condensation nuclei and be washed out by precipitation (in-cloud scavenging) or they can be hit by precipitation below the cloud (below-cloud scavenging). This is called wet deposition.

1.2 Carbonaceous Aerosols

Aerosols consist of different kind of materials such as minerals, sea salt, volcanic SO₂, biological debris, sulfates from biogenic gasses, organic matter from biogenic VOC, nitrates from biogenic NO_x, dust from disturbed soils, soot carbon from biomass burning and fossil fuel burning and nitrates from pollution NO_x. An overview of the most important substances is presented in figure 1.2.

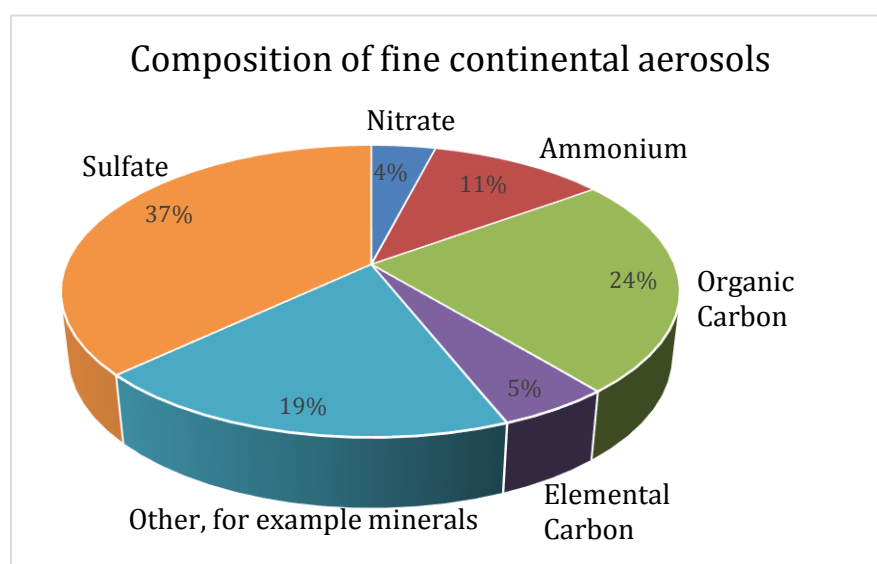


Figure 1.2, composition of fine continental aerosols, data from G.J. Roelofs 2010 and reproduced in a diagram.

Carbonaceous particles are an important fraction in the atmosphere accounting for 20 to 50 percent of all fine particle mass in urban areas (Szidat, 2006). In this thesis the carbonaceous part of aerosols will be investigated. Carbonaceous aerosols have both a direct and indirect effect on climate. They can act as nuclei for cloud condensation, they scatter sunlight and elemental carbon also absorbs longwave and shortwave radiation. They create both positive and negative radiative forcing and positive and negative feedbacks on global warming. According to the IPCC report of 2007 carbonaceous aerosols have an important but yet unknown influence on climate change, due to several positive and negative feedback mechanisms. Numerous studies have shown that carbonaceous particulate matter correlates with severe health effects, including enhanced mortality, cardiovascular, respiratory, and allergic diseases (Keuken, 2013; Mooibroek, 2011; Poschl, 2005).

The organic fraction of an aerosol can be classified using the bottom up- or top down approach. By the bottom up approach every single organic compound has to be identified. This is difficult to achieve because there is a wide range of molecular

structures and only few of them can be investigated at molecular level. Therefore the commonly used method is the top down approach in which total carbon is divided into an organic carbon (OC) fraction and a black carbon (BC) or elemental carbon (EC) fraction. OC is operationally defined as the difference between TC and BC or EC;

$$TC = BC + OC \quad (1.1)$$

$$TC = EC + OC \quad (1.2)$$

Elemental carbon is one of the few particles in the atmosphere capable of absorbing longwave and shortwave radiation. Most of the elemental carbon is anthropogenic of origin due to fossil fuel burning and biomass burning. A smaller part of it originates from nature mostly due to wildfires. It consists primarily of highly polymerized substances having graphite-like structures. Organic carbon can be build up from a mixture of thousands of individual organic compounds from simple alkanes to light polycyclic or poly acidic hydrocarbons (Szidat et al., 2004). EC originates from direct emission and OC can be emitted either as primary (primary organic carbon or POC) or secondary organic aerosol (SOA). Direct OC emission can be man-made, for example cooking or biomass burning, or natural due to plant abrasion or wildfires. Organic carbon can be divided into subgroups; water insoluble organic carbon (WIOC) and water soluble organic carbon (WSOC). Water insoluble organic carbon contains chemical compounds such as polycyclic aromatic hydrocarbons and fatty acid while water insoluble organic carbon consists of polyols, polyethers and several kinds of carbocyclic acids.

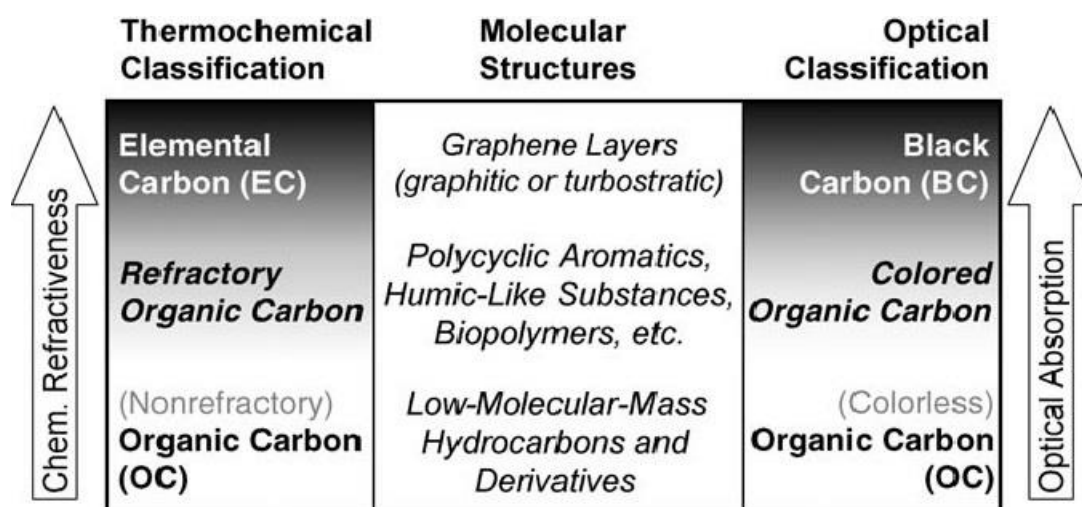


Figure 1.3, organic carbon versus elemental carbon, from Atmospheric Aerosols, U. Pöschl.

As shown in figure 1.3 there is no clear distinction between OC and EC but a gradually increase in optical absorption and refractiveness when going from colorless organic compounds towards black carbon.

1.3 Radiocarbon Measurements

Carbon is the fourth most abundant element by mass after hydrogen, helium, and oxygen in the cosmos. It is also the fifteenth most abundant element on the Earth's crust and found in all known life forms and is the second most plentiful element by mass (about 18.5%) after oxygen in the human body.

The most common isotopes of carbon occurring in nature are ^{12}C , ^{13}C and ^{14}C . The first two are stable but ^{14}C is radioactive and is therefore known as radiocarbon, decaying with a half-life of about 5.730 (+/- 40) years. The first two isotopes are relatively abundant with a share 98,8% and 1,1% in the atmosphere while ^{14}C is present at a very low concentration of $<10^{-10}\%$.

Radiocarbon is produced in the higher layers of the troposphere and in the stratosphere, when cosmic rays produce thermalized neutrons, by hitting atomic nuclei. If a thermalized neutron then hits a nitrogen nuclei it creates ^{14}C as shown in the reaction below;



There are other neutron reactions possible but these are very insignificant, except for the above ground nuclear tests done in the fifties and sixties, and therefore radiocarbon is sometimes called a cosmogenic nuclide. The maximum production rate is at higher latitudes and at a height between nine to fifteen kilometer.

Radiocarbon endures a continuous beta-decay as shown in the following reaction;



One of the neutrons in the radiocarbon atom decays to a proton by emitting an electron (β^{-1}) and an electron antineutrino (ν^*) and the radiocarbon decays into the stable (non-radioactive) isotope N^{14} (nitrogen).

After the creation of ^{14}C ninety-five percent of it transforms further into ^{14}CO . This ^{14}CO is distributed, by the global circulation patterns, over the rest of the world's atmosphere. By reaction with the hydroxyl radical (OH) ^{14}CO can be further transformed into $^{14}\text{CO}_2$ before it enters the main reservoirs like biosphere, ocean and soil. Plants also absorb $^{14}\text{CO}_2$ through photosynthesis and via the food chain it gets into animals and humans.

The actual concentration of ^{12}C , ^{13}C and ^{14}C in the atmosphere is in equilibrium with the concentrations in all living organisms. But as soon as a creature dies, it stops consuming ^{14}C , and because radiocarbon decays over time, the amount of ^{14}C in the organism decreases following the general decay equation;

$$n(t) = n(0)e^{-\lambda t} \quad (1.5)$$

$n(t)$ is the concentration of ^{14}C at time t , $n(0)$ is the concentration of the radioactive compound at time $t=0$ and λ is the radioactive decay constant, which depends on the nuclear species considered and on its way of decay. As mentioned above, the half-life of radiocarbon is 5.730 (+/- 40) years. Lambda is related to the half-life of ^{14}C as follows;

$$\lambda = \frac{\ln 2}{T_{1/2}} \quad (1.6)$$

By measuring the amount of radiocarbon in a dead organism, one is able to calculate the elapsed time since dead. This is the basic idea of radiocarbon dating and is summarized in figure 1.4.

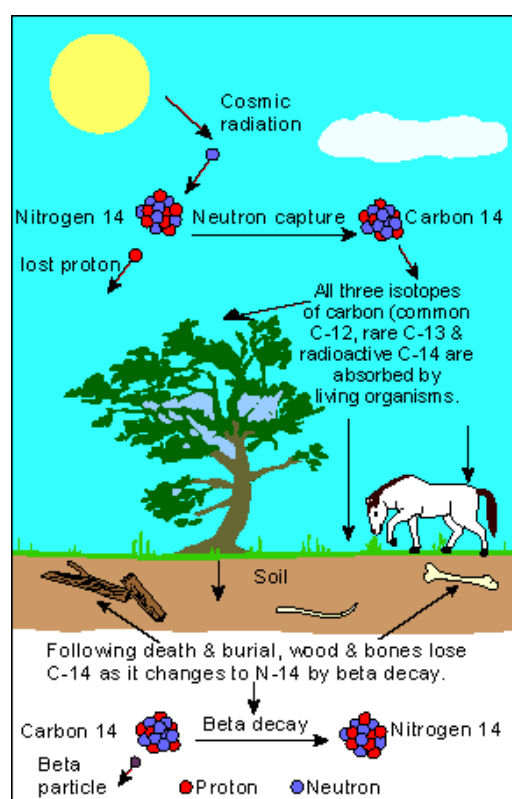


Figure 1.4 cycle of ^{14}C , source; http://www.sciencecourseware.org/virtualdating/files/rc0/rc_0.html

There are two ways of measuring the amount of radiocarbon in aerosols; by counting the amount of radioactive beta-decay of the ^{14}C using gas proportional counters and liquid scintillators detectors. This method was popular in the past and one was capable of working with samples containing grams of carbon.

Today scientists work with accelerator mass spectrometers (AMS) capable of tracing every single ^{14}C atom. With this accuracy only a few micrograms of carbon are sufficient for ^{14}C analysis. Thanks to this progress atmospheric scientists are now capable of measuring the amount of radiocarbon of the different carbon types (TC, EC, OC and WIOC) in aerosols.

This is important because thanks to AMS one is now capable to measure the contribution of anthropogenic fossil fuel burning from cars and factories to the aerosol carbon. It is possible because fossil fuels does not contain ^{14}C , due to the fact that they were buried for millions of years. Therefore anthropogenic fossil fuel burning has its own unique isotopic fingerprint (Röckmann, 2012). On the other hand biomass burning and biogenic processes (from living material like wood, plants and their debris) brings carbon into the atmosphere with roughly the same ratio of $^{14}\text{C}/^{12}\text{C}$ as atmospheric carbon dioxide.

The number of ^{14}C isotopes measured by the accelerator mass spectrometer depends on the ^{14}C concentration but also on the amount of carbon released in the ion source. Therefore the ^{14}C signal is compared with the ^{12}C signal and the final result is presented in a $^{14}\text{C}/^{12}\text{C}$ concentration ratio (Currie, 2000; Szidat et al., 2004c).

The fraction of modern carbon is defined as the actual $^{14}\text{C}/^{12}\text{C}$ ratio compared to that of a reference material and is given by the equation;

$$f_m = \frac{\frac{^{14}\text{C}}{^{12}\text{C}}[\textit{sample}]}{\frac{^{14}\text{C}}{^{12}\text{C}}[\textit{reference}]} \quad (1.7)$$

The reference material is a large batch of oxalic acid, HOxII, measured in the year 1950 and its activity is related to the conditions of plant material. Percent Modern Carbon (pMC) is nothing more than f_m multiplied by a hundred percent (Szidat et al., 2004c).

Over the last century human activities have strongly influenced the $^{14}\text{C}/^{12}\text{C}$ ratio. In the period 1950s-1960s several above ground nuclear bomb tests were done. As a results the $^{14}\text{C}/^{12}\text{C}$ ratio dramatically increased and the amount of radiocarbon in the atmosphere nearly doubled on the tenth of October 1963, see figure 1.5.

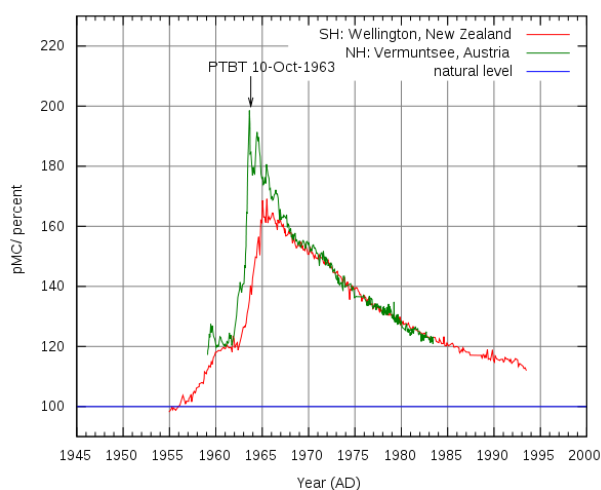


Figure 1.5, atmospheric ^{14}C , in New Zealand and Austria, source; <http://testweb.science.uu.nl/AMS/Radiocarbon.htm>

But due to fossil fuel burning the atmosphere gets enriched with ^{14}C depleted CO_2 (Suess effect). These two developments counteract but nevertheless the bomb signal is strong and this fact should be taken into account.

It is important to realize that trees used as firewood may originate from the period when the nuclear tests occurred. This biomass burning may enrich the atmosphere with ^{14}C again and therefore may influence results as well.

1.4 “Carbonaceous Aerosols; a comparison of different Source Regions, Time Intervals and Meteorological Influences in the Netherlands”

The Netherlands are one of the hotspot areas in Europe with high concentrations of particulate matter. The carbonaceous parts of aerosols are a large fraction of this particulate matter and are influencing both climate and public health. It is therefore important to find out where this carbonaceous particulate matter originates.

The main objective of this thesis is to collect, on a rural site in the Netherlands, total carbon on aerosols. In the laboratory different carbon fractions, total carbon, elemental carbon, organic carbon, water insoluble organic carbon and water soluble organic carbon are extracted from the filters in order to find out if different time intervals, meteorological circumstances or source regions will affect the data.

A thermal extraction system is used to extract the different carbon fractions from the aerosols. Analysis of ^{14}C is used to determine the fossil contribution in the different carbon fractions. A trajectory model is used to determine the source region of the different samples to see if this has an effect on the amount of the different carbon species and their isotopic distribution. Weather data and balloon soundings will reveal any possible meteorological effects on the samples. Different sampling periods and time intervals are tested, for example night and day sampling, to find possible effects on the amount of the different types of carbon and their isotopic composition.

Similar kind of research have been conducted over the years. A short summary of a small number of these results are presented in table 1.1 and 1.2. In table 1.1 the different concentrations of each fraction are shown. For Switzerland, Ireland and Sweden the lowest and highest concentration of each fraction is presented. For the other locations a weighted average is presented. For Yttri (2011) only the concentrations for carbon particles of one micrometer and smaller are shown.

Location	Country	TC, $\mu\text{g per m}^3$	OC, $\mu\text{g per m}^3$	EC, $\mu\text{g per m}^3$	Period	Source
Roveredo, Moleno	Switzerland	7,0 - 33,7	4,9 - 24,2	1,0 - 9,5	January till March 2005	Szidat et al. 2007
Mace Head	Ireland	0,07 - 1,57	0,07 - 1,35		January till november 2006	Ceburnis et al. 2011
Göteborg	Sweden	2,1 - 3,6			winter 2005	Szidat et al. 2009
Göteborg	Sweden	2,2 - 3,0			summer 2006	Szidat et al. 2009
Aveiro	Portugal	14,10	12,30	1,80	winter 2002 and winter 2003	Gelencsér et al. 2007
Aveiro	Portugal	4,04	3,47	0,57	summer 2002 and summer 2003	Gelencsér et al. 2007
Puy de Dôme	France	0,86	0,65	0,21	winter 2002 and winter 2003	Gelencsér et al. 2007
Puy de Dôme	France	4,92	4,63	0,29	summer 2002 and summer 2003	Gelencsér et al. 2007
Schauinsland	Germany	1,66	1,38	0,28	winter 2002 and winter 2003	Gelencsér et al. 2007
Schauinsland	Germany	4,05	3,80	0,25	summer 2002 and summer 2003	Gelencsér et al. 2007
Sonnblick	Austria	0,21	0,19	0,02	winter 2002 and winter 2003	Gelencsér et al. 2007
Sonnblick	Austria	1,56	1,44	0,12	summer 2002 and summer 2003	Gelencsér et al. 2007
K-Pusztá	Hungary	10,70	8,91	1,74	winter 2002 ,winter 2003,winter 2004	Gelencsér et al. 2007
K-Pusztá	Hungary	5,04	4,52	0,53	summer 2002 and summer 2003	Gelencsér et al. 2007
Oslo	Norway		2,50	0,46	summer 2006	Yttri et al. 2011
Oslo	Norway		2,19	0,78	winter 2007	Yttri et al. 2011
Hurdal	Norway		2,60	0,27	summer 2006	Yttri et al. 2011
Hurdal	Norway		1,32	0,27	winter 2007	Yttri et al. 2011

Table 1.1, concentration of the different fractions. For Switzerland, Ireland and Sweden the lowest and highest concentration of each fraction is presented. For the other locations a weighted average is presented. For Yttri (2011) only the concentrations for carbon particles of one micrometer and smaller are shown. The other results are for particles smaller than 2.5 micrometer.

In table 1.2 the fraction modern of the different carbon fractions are presented. The minimum and maximum value of the different sites are shown.

Location	Country	TC, f_m in %	OC, f_m in %	EC, f_m in %	Period	Source
Roveredo, Moleno	Switzerland		0,697 - 1,098	0,171 - 0,909	January till March 2005	Szidat et al. 2007
Mace Head	Ireland	0,634 - 0,889	0,719 - 0,937		January till november 2006	Ceburnis et al. 2011
Göteborg	Sweden		0,63 - 0,74	0,08 - 0,15	winter 2005	Szidat et al. 2009
Göteborg	Sweden		0,59 - 0,78	0,05 - 0,17	summer 2006	Szidat et al. 2009

Table 1.2, fraction modern for TC, OC and EC as measured on several European sites. The minimum and maximum fraction modern of each carbon fraction is shown.

2. Methodology

2.1 Location

The aerosols were collected with a High Volume sampler near Cabauw at the CESAR observatory field. This field is situated in a polder, 0.7 m below sea-level, in the western part of the Netherlands (51.971° North, 4.927° East).

A big advantage of this site is that within 25 kilometer of the station there is a regular radiosonde location at De Bilt and the landscape is also rather representative for most of the Netherlands. As we can see in figure 2.1 the area is rural with just a few villages and some agricultural activities, the landscape is flat with a maximum surface elevation difference of just a few meters in the surrounding area but one kilometer to the southeast there is a dike and the river Lek where several cargo boats pass every day. In between the dike and the sampler there is also a provincial road. The North Sea is more than 45 kilometer (Google maps) away to the west-northwest. Though the High Volume Sampler is on a rural site it is also surrounded by big cities as Utrecht, Rotterdam, Den Haag and Amsterdam thirty to forty kilometers away. These cities are connected with big highways which, at a distance, surrounds Cabauw. As a result pollution levels on this rural site are high compared to other rural sites in Europe.

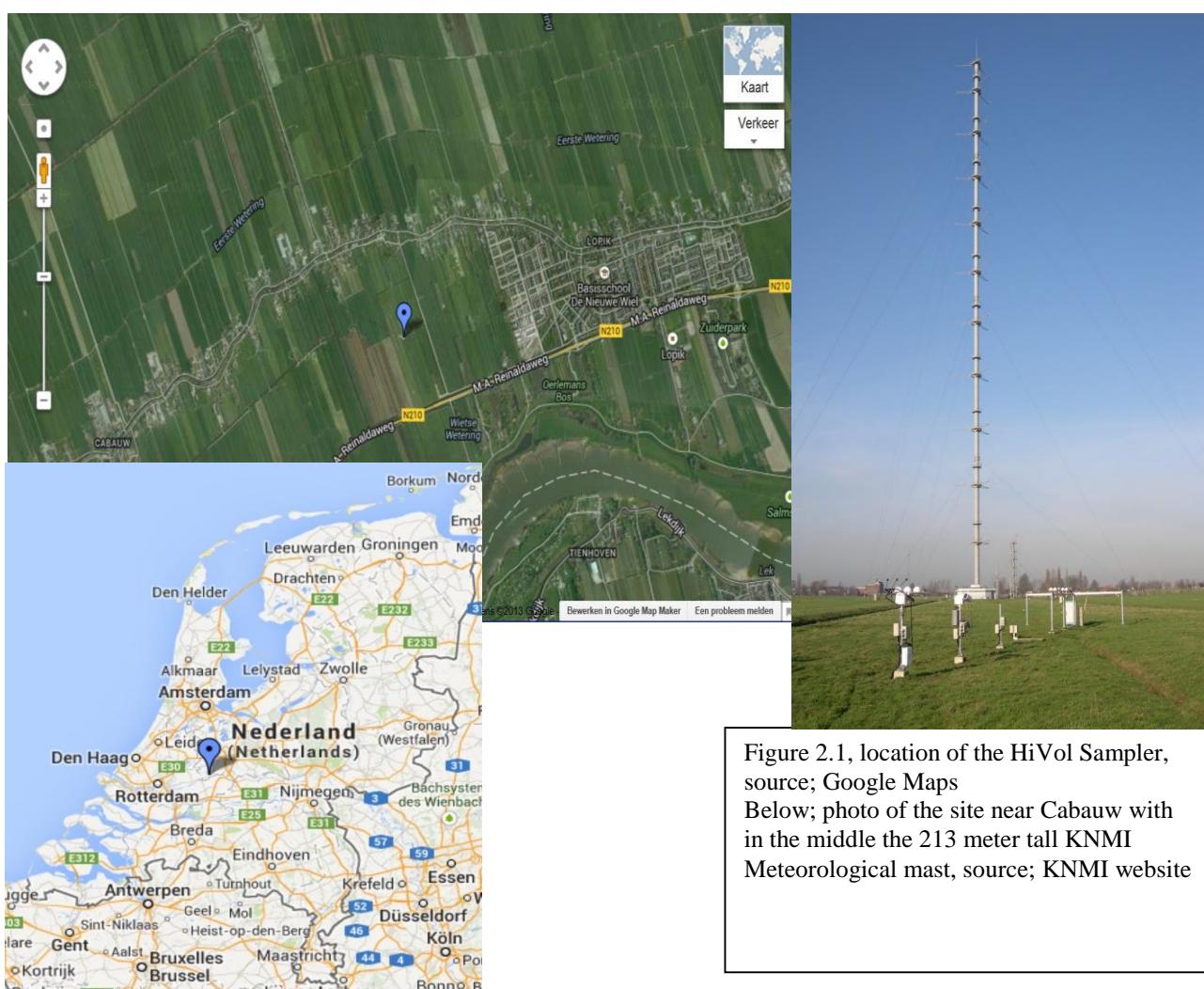


Figure 2.1, location of the HiVol Sampler, source; Google Maps
Below; photo of the site near Cabauw with in the middle the 213 meter tall KNMI Meteorological mast, source; KNMI website

2.2 High volume Sampler

At the Cabauw site a high volume sampler, Digitel HVS model DHA 80, is used to collect the aerosols. Like a vacuum cleaner it sucks air through a filter which collects the aerosols, see figure 2.2.

A blower creates a steady airflow, from top to bottom, through the sampler. The air flows at the top of the device through a PM_{2.5} inlet (1) system. This inlet removes particulate matter with an aerodynamic diameter larger than 2.5 μm . Inside the inlet the airstream is channeled through ten small tubes arranged in a circle. These tubes leads the airstream to an impactor plate. This impactor plate is a circular aluminum plate covered with grease, see figure 2.3. Large particles cannot follow the airflow and are dropped on the grease layer. This impactor plate usually needs to be cleaned every two weeks.

The flow continue to the flow chamber (2) and here the air goes through spherical quartz fiber filters (Whatman, QMA(3)) with a diameter of 150 mm (the filter diameter exposed to the flow is 140 mm due to the filter-holder on which the filter is attached) on which the aerosol particles are collected. The filter holder is a circular with a diameter of 180 millimeter and is composed of an air permeable grid on which the filter is placed and a thin teflon ring surrounding the filter edge.

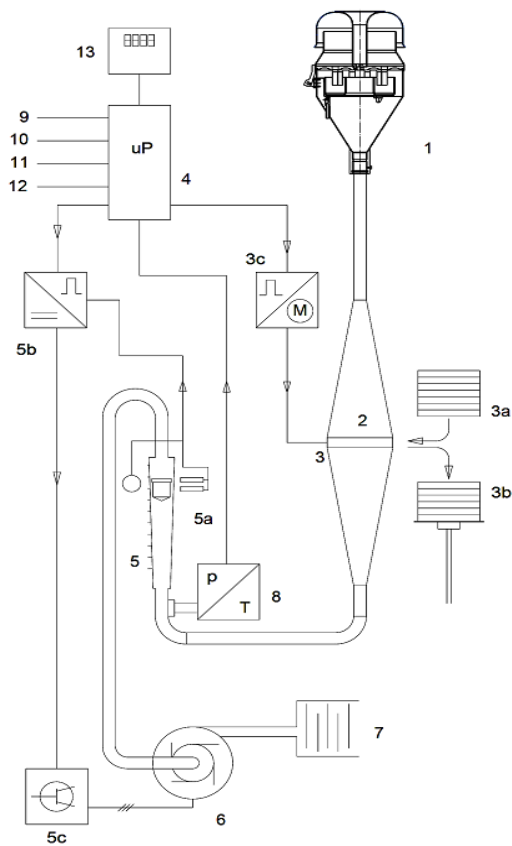
A microprocessor control unit (4) collects data about air pressure and temperature inside and outside the high volume sampler and the volume flow of air which is measured optically with a floater (5a) in a tube. The flow is kept constant at 500 liter/min for a good reproducibility and long-term stability. The control unit is also used for time controlled measurements in which day and night filters were changed automatically at 7 p.m. and 7 a.m. Filter-holders were changed automatically, steered by the control unit, with a mechanical arm. New filter-holders where grabbed from the filter stock (3a) and put in the filter holder place (3) where the filter collects aerosols once the air flow has started. Old filter-holders are pushed automatically to the filter-holder storage when the collection is completed (3b).

2.3 Filter preparation

During filter preparation everything is done to avoid organic contamination. The new quartz fiber filters are pre-heated in an oven at 800 degrees Celsius overnight. After that they are folded in aluminum foil, packed into air-tight plastic bags and put in a freezer at minus 20 degrees Celsius. The aluminum foils themselves are pre-heated in an oven at 500 degrees Celsius for at least three hours. Tweezers necessary during the process were pre-cleaned with ethanol.

On the day of a new measurement the filter-holder and Teflon ring are cleaned with ethanol, since both parts are directly in contact with the filter. Once the ethanol is completely evaporated the filter can be inserted in the holder and is ready for sampling in the High Volume Sampler.

After sampling the quartz fiber filters are folded again in aluminum foil, packed into air-tight polyethylene bags and put in a freezer at minus 20 degrees Celsius for later off-line analysis.



- 1 inlet
- 2 flow chamber
- 3 current filter
- 3a filter stack
- 3b used filters
- 3c exchange electronics
- 4 control
- 5 flow meter
- 5a flow sensor
- 5b flow control
- 5c frequency converter
- 6 blower
- 7 noise baffle
- 8 pressure and temperature measurement unit
- 9 printer interface
- 10 RS-232C interface
- 11 Ethernet
- 12 USB
- 13 touch screen control panel

Figure 2.2, upper left the high volume sampler, upper right a dirty aluminum impactor plate. And a technical sketch of the high volume sampler, sources; Digital DHA-80 Product Datasheet, Monaco.

2.4 Thermal Extraction of OC and EC

As described in the first chapter OC and EC have different thermal properties. OC is combusted at a lower temperature than EC and this principle can be used to separate the different carbon fractions. In order to separate EC more accurately from OC the filters are water-extracted before separating EC and water insoluble organic carbon (WINSOC) as shown in figure 2.3.

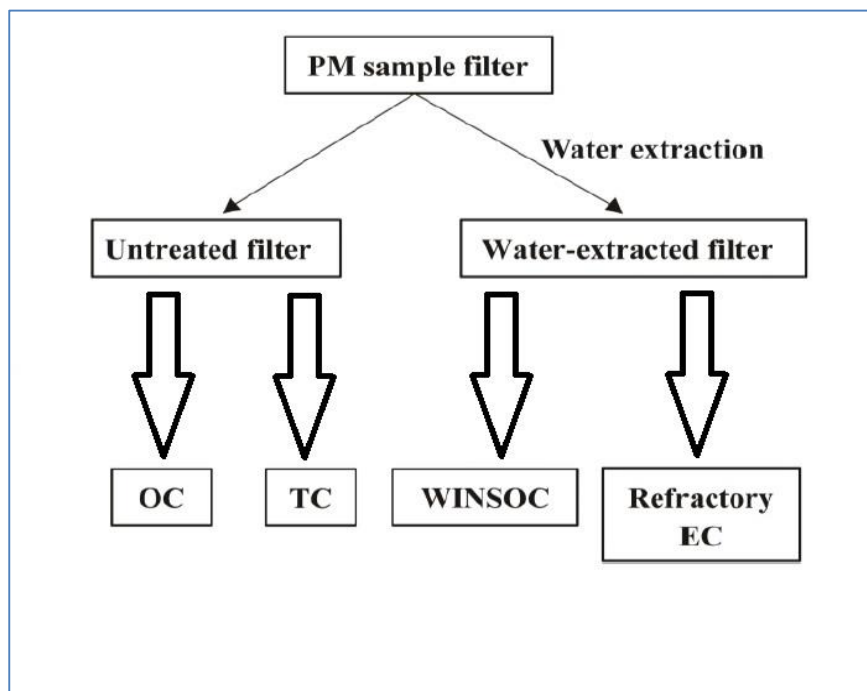


Figure 2.3, separation scheme of the different carbon fractions for ^{14}C measurement, source Zhang 2012, modified.

The thermal extraction method is based on the THEODORE (Two-step Heating system for the EC/OC Determination Of Radiocarbon in the Environment) system from Szidat (Szidat et al., 2004c). And has been further developed over the years at the Institute of Marine and Atmospheric research Utrecht (Derendorp, 2007; Prokopiou, 2010; Gongriep, 2011; Monaco 2011).

The thermal setup currently used at IMAU is shown in figure 2.4. Schematically the system can be divided into two sub-systems: the reaction tube, where the filter combustion and CO_2 formation occurs and the glass line, where carbon dioxide is collected, cleaned and stored. These two are separated by a needle valve (D) that controls the flow through the reaction tube and regulates the pressure in both reaction tube and glass line.

The reaction tube (C) is coupled with two gas lines, one with pure helium (He) and another one with oxygen (O_2), the two purple ovals in figure 2.4. To avoid any contamination the two gasses are further purified before reaching the reaction tube. First of all they pass an oven (A) which, at 850°C , oxidizes possible traces of carbon monoxide and hydrocarbons into carbon dioxide (CO_2) using nickel oxide wires as a catalyst. Then the gasses go through a potassium hydroxide (KOH) filter (B) where water vapor and carbon dioxide are removed from the helium or oxygen.

For safety and standardization of the process a mass flow controller is used to control the oxygen flow. Helium, a noble gas, is used to flush the system before a sample is placed in the reaction tube while oxygen is needed for the creation of carbon dioxide during the combustion process.

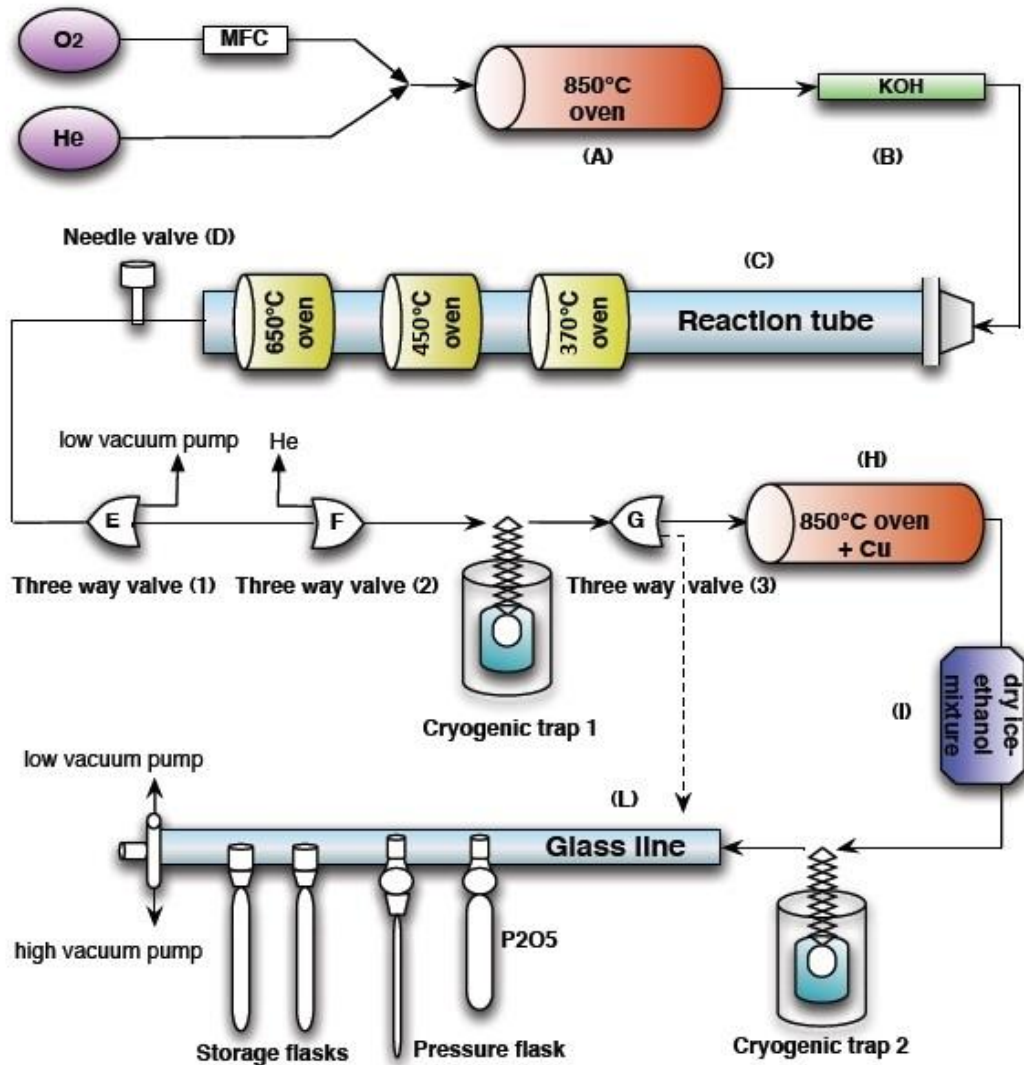


Figure 2.4, current setup of the thermal system at IMAU, source Monaco, modified.

After the whole system has been evacuated to remove any contamination, the reaction tube is filled with helium with a slight overpressure. This prevents any new contamination from entering the reaction tube. For OC extraction a circular piece of the filter (area of the cutter is 7.07 cm²) is put on a sample holder and placed in the reaction tube in front of the ovens. Then the reaction tube is flushed with helium for ten minutes to remove the ambient air that went into the system after inserting the filter. Meanwhile cryogenic trap 1 is cooled with liquid nitrogen. The gas valve is switched to O₂. After 5 minutes the whole system is filled with O₂ and the sample is pushed, by magnets, into the first oven at 370°C. It will stay in the oven for 15 minutes, the O₂ flow is kept constant at 55 ml per minute, burning the OC and turning it into CO₂. Meanwhile a cryogenic trap containing dry ice and ethanol (I) is placed after the copper oven (H). This mixture, with a temperature of minus 70°C, is

collecting H₂O further in the process. The CO₂ is caught in cryogenic trap 1. After 15 minutes three way valve E is switched to low vacuum pump and the glass line is evacuated with low and high vacuum to remove all oxygen. Meanwhile cryogenic trap 2 is cooled with liquid nitrogen. The high vacuum pump is closed again and helium is flushed in via valve F and trap 1 is quickly heated with an industrial dryer. The gas now flows through the copper oven and the ethanol/dry ice trap to remove NO_x and H₂O. After ten minutes the valve is closed and the glass line is evacuated for twelve minutes with the vacuum pumps to remove all helium. Then the gas is cryogenically moved to the P₂O₅ flask where it is stored for 5 minutes in order to remove the remaining H₂O gas. Then the purified CO₂ is cryogenically trapped in the pressure flask, a calibrated volume with pressure sensor for determination of the extracted amount of CO₂. The mass of the trapped carbon, in micrograms, is calculated with use of the ideal gas law;

$$PV = nRT \quad (2.1)$$

where P is the pressure measured in the flask, V is the volume of the flask (2,5 ml), n is the number of moles, R is the ideal gas constant (8,314472 J/K mol) and T is the measured temperature which was relatively constant at 303 Kelvin. After calculating the number of moles the mass is known;

$$m = Mn \quad (2.2)$$

where m is the mass of carbon (in microgram), M is the molar mass (12,0178 gram/mol) and n the calculated number of moles. The mass of carbon on the filter can now be calculated. This mass is then divided by the air volume of the samples to retrieve the aerosol concentration in µg/m³.

After measuring the pressure the CO₂ is cryogenically trapped in a break seal tube and the glass line is evacuated with the low and then the high pressure vacuum pump. The break seal is burned off the glass line and stored for later analysis of ¹⁴C. During the thermal extraction of OC it is possible that some EC is also oxidized during the OC step, leading to an underestimation of this EC fraction (Zhang, 2012). Because wood-burning EC was reported to be the least refractory EC fraction this underestimation could occur in periods when there is lot of biomass burning.

For the extraction of TC the same procedure is followed as by OC except now the sample piece is put in oven two at 650 degrees Celsius.

By the thermal extraction of EC there is a risk of pyrolysis of OC which is called charring. To minimize charring the sample piece is water extracted to remove Water Soluble Organic Carbon abbreviated as WSOC, as suggested from prior study results (Prokopiou, 2010; Gongriep, 2011; Monaco, 2012; Zhang, 2012). Just like for OC and TC a circular piece is cut from the filter (area of the cutter is 7.07 cm²).

The filter piece is soaked in pure milli-Q (ultrapure, type 1) water, see figure 2.4, (14 ml per filter piece) overnight and dried for 48 hours in an air-tight desiccator. Thus the water-soluble organic compounds, responsible for most of the charring, are removed and only the water insoluble organic carbon (WIOC) remains on the filter.

A similar procedure as described above is followed by OC and TC, but this time the filter piece is put in the first oven at 370°C to oxidize and trap WIOC. To remove the remaining WIOC the sample is placed in the second oven at 450°C for two minutes.

Later in the process the sample is put in the second oven again at 650°C for 15 minutes to burn and cryogenically trap the EC.



Figure 2.5, a filter piece soaked in milli-Q water, source Monaco.

In appendix A the exact procedure followed in this thesis to extract TC, EC, OC, WOIC and the removal of OC en WIOC are described. The overall error margin of the whole thermal extraction system is unknown and should be investigated. Therefore no error margin could be displayed.

The flasks of TC, OC, WIOC and EC obtained in this manner were send to Groningen and Zurich. At Groningen and Zurich accelerator mass spectrometers were used to determine the fraction modern of the different carbon fractions as described in paragraph 1.3. The error margin ranged from 0,2% till 1,2%. These values are so small that they could not be shown in the graphs.

2.5 Meteorological Data

Meteorological conditions during sampling might influence the amount of particulate matter of the different species or the fraction modern of the several carbon fractions. Therefore the maximum and minimum temperature in degrees Celsius, wind direction at 10 meter height in degrees, wind speed in kilometers per hour, relative humidity in percentage and a synoptic overview including location of high and low pressure centers and precipitation are reported. Relative humidity is also used to calculate boundary layer height with a skew-t diagram, see figure 2.8.

Local meteorological conditions at the Cabauw site were retrieved from the KNMI (Royal Netherlands Meteorological Institute) website. Their weather station is located approximately 20 meters east-northeast of the high volume sampler.

Balloon soundings were used to determine meteorological circumstances higher in the atmosphere, inversion layers and boundary layer height for example might influence particulate matter and fraction modern.

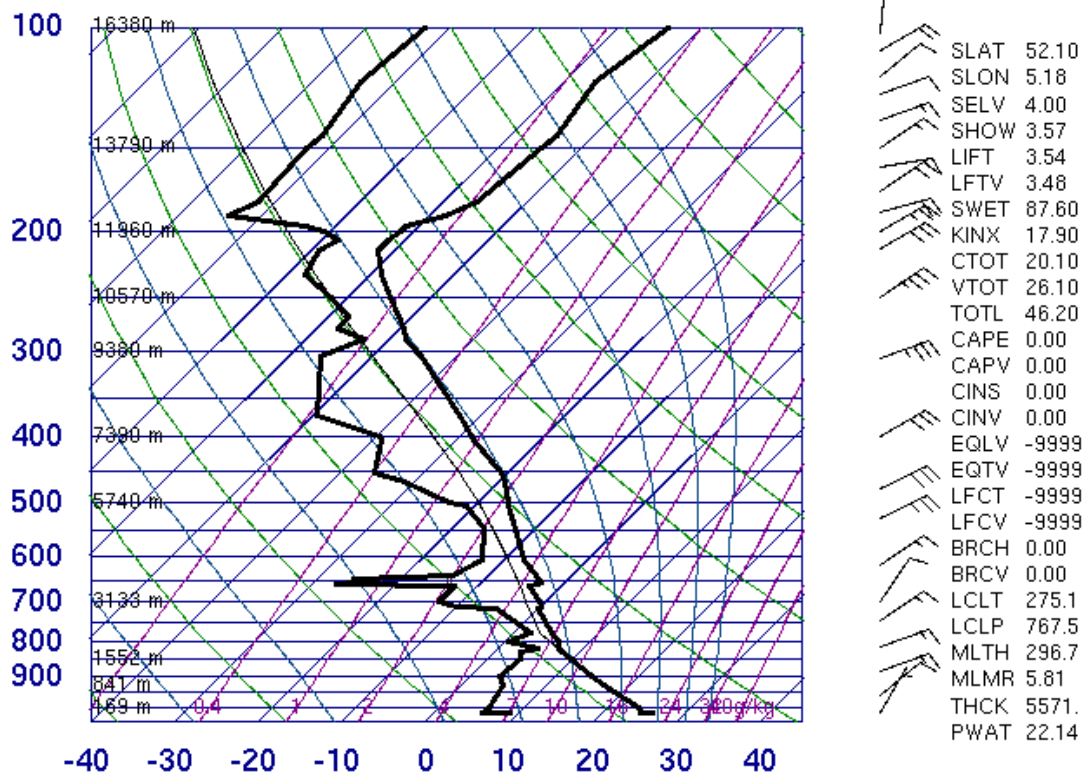
Every day at 00:00 and 12:00 Universal Time a KNMI weather balloon is launched at De Bilt. De Bilt is 25 kilometers (Google maps) east of the high volume sampler. The results are sent by radio to De Bilt therefore weather balloons are also called radiosondes. The probe typically reaches a height of between 17 and 25 kilometers. During the flight, which lasts up to two hours, measurements of temperature, humidity and air pressure are done. From the position of the probe the wind speed and direction is calculated. The data of the sounding is plotted in a skew-t diagram, see figure 2.6. These soundings are an important tool in this thesis to determine the boundary layer height and possible inversion layers because these might influence particulate matter concentration. Hence it is reported in the thesis whether the atmosphere was stable or convective and how high the convection or convective clouds would go, what the depth was of the mixed layer height and at what height inversion layers were found, in meters, to find the “ceiling” of the atmosphere during sampling.

In a skew-t diagram the following sets of lines can be found;

1. Dry adiabats, curved lines to describe the temperature change a dry air parcel would have if it was raised adiabatically in the troposphere.
2. Moist adiabats, curved lines to describe the temperature change a saturated air parcel would have if it was raised adiabatically in the troposphere.
3. Isotherms, solid lines with a 45 degrees angle, of constant temperature.
4. Isohumes, lines of equal relative humidity in gram water vapor per kilogram air.
5. Isobars, horizontal lines of constant pressure in hectopascal.

First of all the lowest inversion levels are determined with the skew-t diagram. It is important to know this height because the aerosols might be trapped under a low ceiling resulting in high concentrations. In this thesis an inversion level is a level in the atmosphere where air temperature is higher than just below this inversion layer. In figure 2.6 for example we find an inversion layer at approximately 650 hectopascal. But as a result of strong convection from the ground or at higher levels or due to forced lifting the inversion layer(s) might be crossed.

06260 EHDB De Bilt



12Z 27 May 2012

University of Wyoming

Figure 2.6, example of a skew-t diagram used in this thesis. Blue horizontal lines are isobars. The green curves lines are dry adiabatic lapse rates, the blue curved lines are moist adiabatic lapse rates, the purple straight lines are isohumes and the blue solid lines sloped at 45 degrees are isotherms, the black thick solid line on the right is temperature and the black thick solid line on the left is the dewpoint temperature, source <http://weather.uwyo.edu/upperair/sounding.html>

Therefore convection is also taken into account. From the KNMI weather data the two meter level temperature and dew point temperature are known. This is used in the skew-t diagram by following from the surface dew point temperature the appropriate isohume (lines of equal relative humidity) in its ascend along the line until the ambient air temperature, thick black solid curve, is crossed. This is the convective condensation level at which cloud base formation could occur if the specific level can be reached by an ascending air parcel from the ground. Following the dry adiabat down to the surface reveals the surface temperature or convective temperature at which condensation at the convective condensation level will occur. If this surface temperature is reached and thus condensation occurs latent heat from condensation is released and the moist adiabatic lapse rate is followed upwards, from the convective condensation level, towards the point where the moist adiabatic curve cross the black ambient temperature line. At this point the equilibrium level (EL) or cloud top level is reached which is, in this thesis, considered to be the boundary layer height.

In case of forced lifting, due to fronts, the correct isohume and dry adiabat are followed upwards until the point where the two lines cross. This is called the lifting condensation level from where the moist adiabat is followed in case the air parcel is warmer and less dense than the surrounding air. Cloud top level and boundary level are determined in a similar way as in the case of convection from the ground.

2.6 Trajectory Model

One can imagine that air masses from different source regions, for example industrial areas, rural background, North Sea or Swedish forests will result in different aerosol composition related to air mass history. It is therefore very interesting to investigate the differences in carbon concentrations and isotopic composition depending on the air trajectory. NOAA HYSPLIT trajectories (<http://ready.arl.noaa.gov/HYSPLIT.php>) are used to plan the sampling in order to sample comparable air masses from a specific part of the continent on each particular filter. This information is used to understand differences in aerosol composition related to air mass history. For this thesis 72 hours back trajectories are used.

In figure 2.7 an example of a trajectory is presented. Sample CA 99 was collected from January 20 till January 23 2012. Each day a trajectory was started at 12:00 UTC in the afternoon. So there are 4 trajectories and everyday has its own color. For example the trajectory started at January 23 is red and the trajectory started at January 21 is green. The trajectory is backwards in time and for every 24 hours back in time a symbol (square or triangle) is displayed in the figure.

In the upper part of figure 2.7 a map is presented to show the position of the trajectory. In the lower part of figure 2.7 one can see the height of that trajectory. For example the trajectory that ended on January 23 near the high volume sample (red) was 72 hours back in time (on January 20, 12:00 UTC) above Greenland at a height of approximately 2800 meters. And a day later the air was on the Atlantic ocean at a height of approximately 1400 meters.

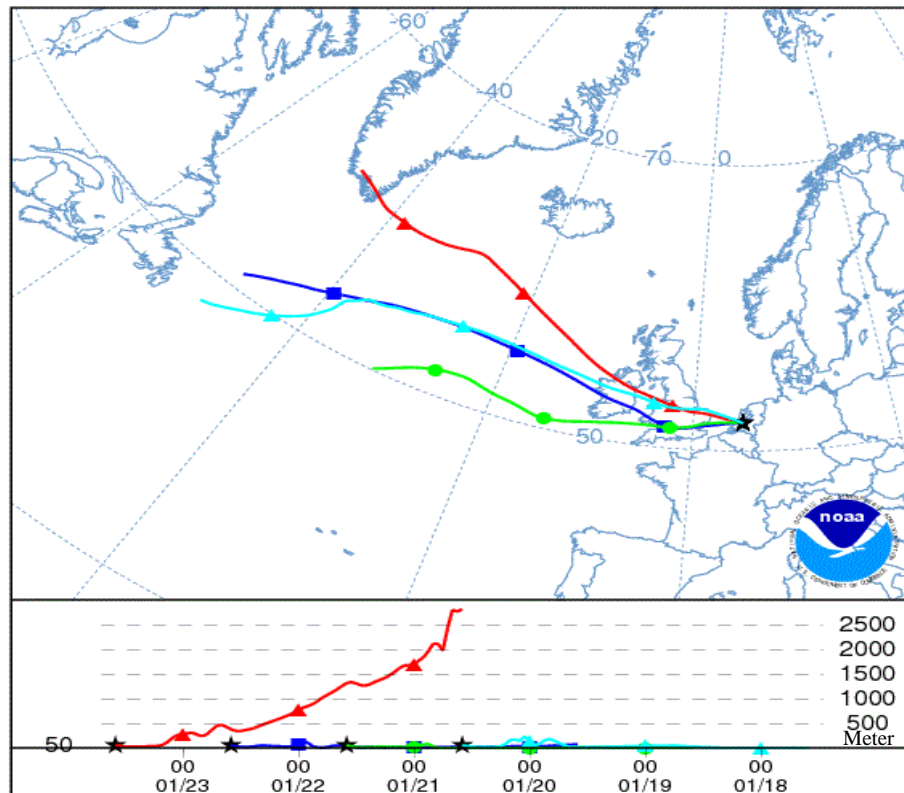


Figure 2.7, example of the Hysplit trajectory model in this case sample CA 99. Everyday a new trajectory was started at 12:00 UTC. And every trajectory has its own color. In the upper part of the figure a map is showing the position of the trajectory. In the lower part the height of the trajectory in meters is shown. Source; <http://ready.arl.noaa.gov/HYSPLIT.php>

2.7 Overview of collected samples

The main objective of this thesis is to analyze the amount and isotopic composition of carbonaceous aerosols at a rural site in the Netherlands, in order to find out if they are affected by different diurnal patterns. The samples are collected during periods in which the air mass history was rather constant and different air masses could be identified. In table 2.1 the fall/winter samples used in this thesis are shown.

sample code	date start	date end	filter type
CA 84A	14-Nov-2011 11:30	17-Nov-2011 15:30	Front
CA 85A	17-Nov-2011 15:30	21-Nov-2011 18:00	Front
CA 99	20-Jan-2012 18:05	23-Jan-2012 15:50	Single
CA 102	30-Jan-2012 19:50	3-Feb-2012 14:00	Single
CA 106	13-Feb-2012 12:05	16-Feb-2012 17:00	Single
CA 109	1-Mar-2012 12:35	7-Mar-2012 18:45	Single

Table 2.1, list of collected fall/winter samples.

CA stands for Cabauw with increasing numbers over time. When two filters in one filter-holder are used, the front filter is on top, resting on the back filter while the back filter lays on the filter-holder. The back filters were not used in this thesis. By a single filter only one filter in a filter-holder is used. In table 2.2. the day and night filters are listed.

sample code	date start	date end	filter type
CA 118C	17-May-2012 19:00	20-May-2012 07:00	Field Blank
CA 119A	17-May-2012 19:00	20-May-2012 07:00	Front Night
CA 119B	17-May-2012 19:00	20-May-2012 07:00	Back Night
CA 120A	18-May-2012 07:00	20-May-2012 12:00	Front Day
CA 120B	18-May-2012 07:00	20-May-2012 12:00	Back Day
CA 122A	25-May-2012 07:22	27-May-2012 19:22	Front Day
CA 122B	25-May-2012 07:22	27-May-2012 19:22	Back Day
CA 123A	24-May-2012 19:22	27-May-2012 07:22	Front Night
CA 123B	24-May-2012 19:22	27-May-2012 07:22	Back Night
CA 124	24-May-2012 19:22	27-May-2012 19:22	Field Blank
CA129A	1-Jul-2012 07:00	3-Jul-2012 19:00	Front Day
CA 129B	1-Jul-2012 07:00	3-Jul-2012 19:00	Back Day
CA 130A	30-Jun-2012 19:00	3-Jul-2012 07:00	Front Night
CA 130B	30-Jun-2012 19:00	3-Jul-2012 07:00	Back Night
CA 131	30-Jun-2012 19:00	3-Jul-2012 19:00	Field Blank
CA 133A	12-Jul-2012 07:00	13-Jul-2012 19:00	Front Day
CA 133B	12-Jul-2012 07:00	13-Jul-2012 19:00	Back Day
CA 134A	11-Jul-2012 19:00	13-Jul-2012 07:00	Front Night
CA 134B	11-Jul-2012 19:00	13-Jul-2012 07:00	Back Night
CA 135	11-Jul-2012 19:00	13-Jul-2012 19:00	Field Blank

Table 2.2, list of collected day/night filters.

The night filter collects aerosols from 19:00 till 7:00 and the day filters from 7:00 till 19:00. The filters were manually put back in the filter stock for the following day.

2.8 Correction of fraction modern

The carbon found on an aerosol filter includes the actual aerosol sample as well as the contamination introduced through filter handling, transport, and storage. Therefore field blanks and handling blanks are collected to characterize the contamination on filter samples. Field blanks are used to correct day/night filters because field blanks are in the filter-holder storage during the entire sampling period and day night filters are in the filter-holder storage during half of the sampling period.

Handling blanks are used to correct the fall/winter filters because these filters during the entire sampling period in the active air flow and a handling blank goes through the sampling system without collecting aerosols in the active air flow.

By a field blank, a filter for a blank experiment is stored inside the high volume sampler during the sampling period but outside the active airflow. It does not actively collect aerosols, but it is placed in the filter-holder storage passively collecting particles and gases inside the high volume sampler box. By a handling blank, a filter for a blank experiment is grabbed from the filter stock and put in the filter holder place where the filter collects aerosols and gases, but before the air flow starts it is pushed automatically to the filter-holder storage. After the handling blank went through the high volume sampler, the “active” filter is positioned in the filter holder place.

The handling blank is used to correct the measured carbon amount and fraction modern as follows. The measured carbon (M) on any filter is given as the sum of the aerosol carbon (S) and the contamination, which is the carbon amount measured on a blank filter (B);

$$M = S + B \quad (2.3)$$

In order to get the corrected fraction modern (f_m) the following formula is used;

$$f_{m(S)} = \frac{f_{m(M)} * M - f_{m(HB)} * HB}{(M - HB)} \quad (2.4)$$

where HB stands for handling blank.

Day/night filters are not in the airflow during the entire sampling period, fifty percent of the time they are in the filter holder storage. To correct for the resulting contamination field blanks are used. But field blanks are in the filter holder storage during the entire sampling period. Therefore the amount of carbon (TC, OC) found on the field blank is divided by two;

$$f_{m(S)} = \frac{f_{m(M)} * M - f_{m(FB)} * \frac{1}{2}FB}{(M - \frac{1}{2}FB)} \quad (2.5)$$

where FB stands for field blank. For elemental carbon the correction is done with the handling blank using formula 2.4 because the amount of elemental carbon on the field blank does not increase in time.

3. Results

In this chapter the results of the different sampling campaigns are shown. The results of the fall/winter samples are presented in the first paragraph followed by the day/night filters in the second paragraph. As described in paragraph 2.4 the error from ^{14}C measurements was too small to be displayed and the overall error of the thermal extraction system was unknown.

3.1 Fall/winter Samples

Sample CA 84A was collected in the period from 14 November till 17 November 2011. The results are presented in figure 3.1.

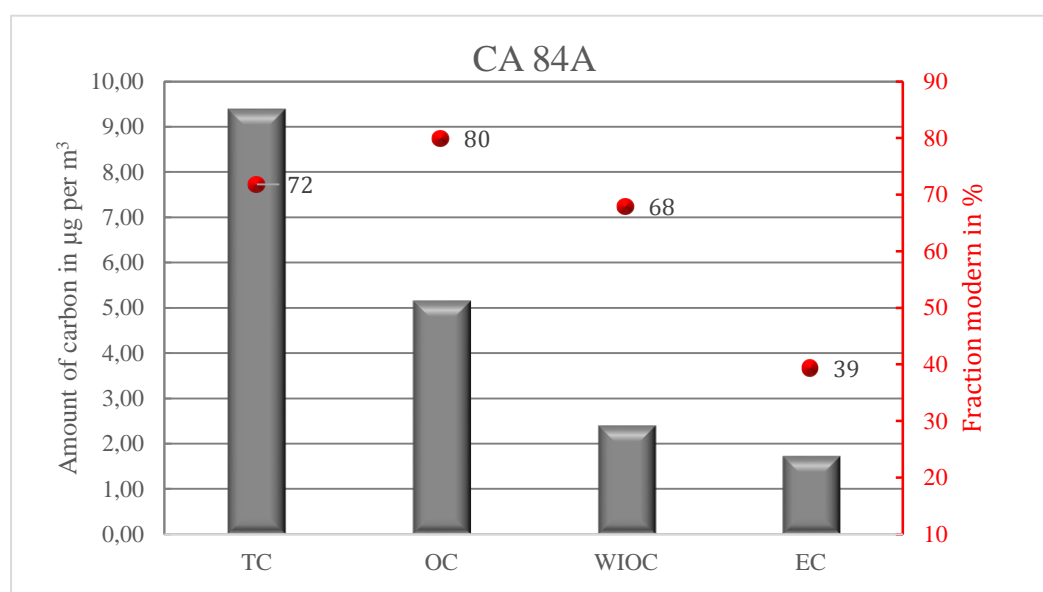


Figure 3.1, the amount of the different carbon fractions and fraction modern of sample CA 84A.

In figure 3.1 the grey bars indicate the concentration of the different carbon fractions (TC, OC, WIOC and EC) in microgram carbon per cubic meter. The amount of carbon in $\mu\text{g per m}^3$ are shown on the left y axis. During the sampling period the concentration of total carbon measured in the atmosphere was $9,4 \mu\text{g m}^{-3}$ carbon per cubic meter. The largest fraction was OC followed by WIOC and EC.

The red dots in figure 3.1 show the fraction modern of the corresponding carbon fractions. The units are shown on the right y axis. OC had a relatively high fraction modern of 80 percent, followed by WIOC with 68 percent. EC had, with 39 percent, the lowest fraction modern.

In figure 3.2 the three day back trajectories corresponding to sample CA 84A are shown. At the beginning of the sampling period the air went over Austria and Germany towards the station. This lasted two days and then the air mass came from Poland and went over the Czech Republic and Germany. On the last sampling day the air mass came from the Gulf of Genoa and went over France and Belgium before it reached the high volume sampler.

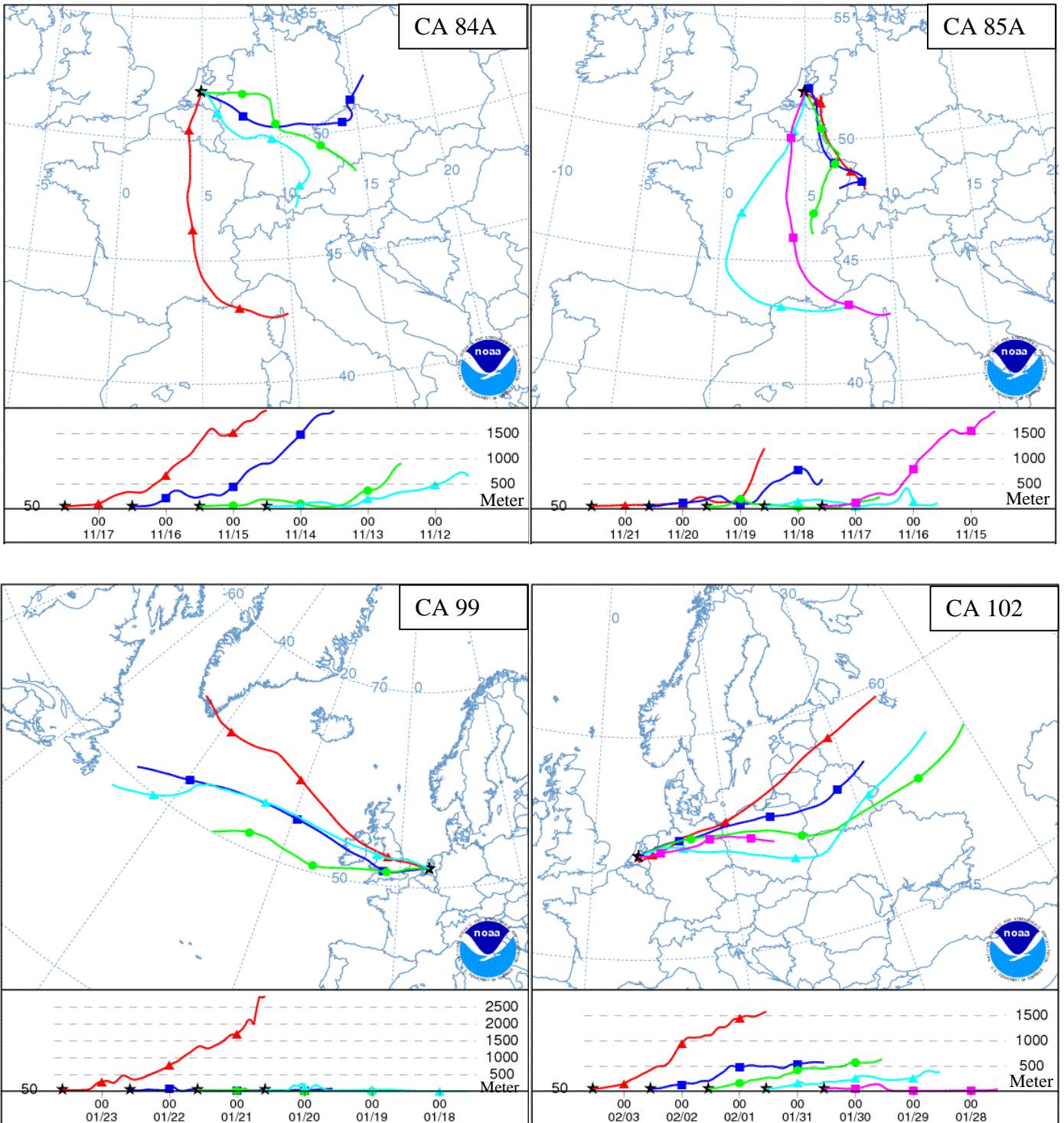


Figure 3.2, an overview of trajectories of samples CA 84A (November 14 till November 17 2011, upper left), CA 85A (November 17 till November 21, upper right), CA 99 (January 20 till January 23 2012, left) and CA 102 (January 30 till February 3 2012, right), source; <http://ready.arl.noaa.gov/HYSPLIT.php>, but modified.

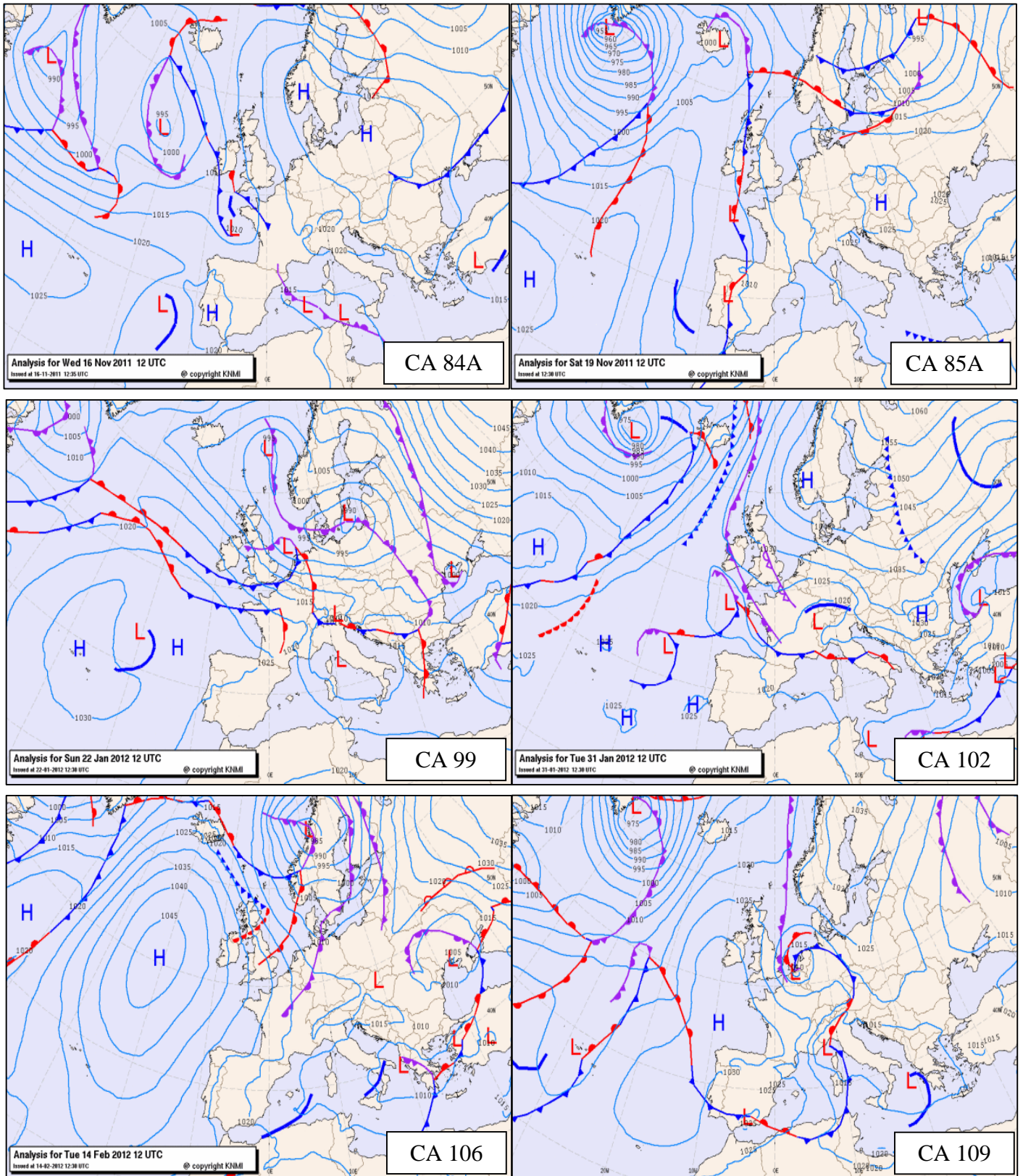


Figure 3.3, synoptic analyses of the different pressure systems and fronts during the different sampling periods. Source, KNMI, www.knmi.nl, modified.

At Cabauw a high pressure system with its core over eastern Europe was dominating the weather and it remained dry. During the period the wind went from east to south, allowing moist air from the sea to mix with the drier continental air. In figure 3.3 a synoptic overview of the pressure systems on November 16 is given.

Sample CA85 A was collected from 17 November till 21 November 2011. The results are presented in figure 3.4.

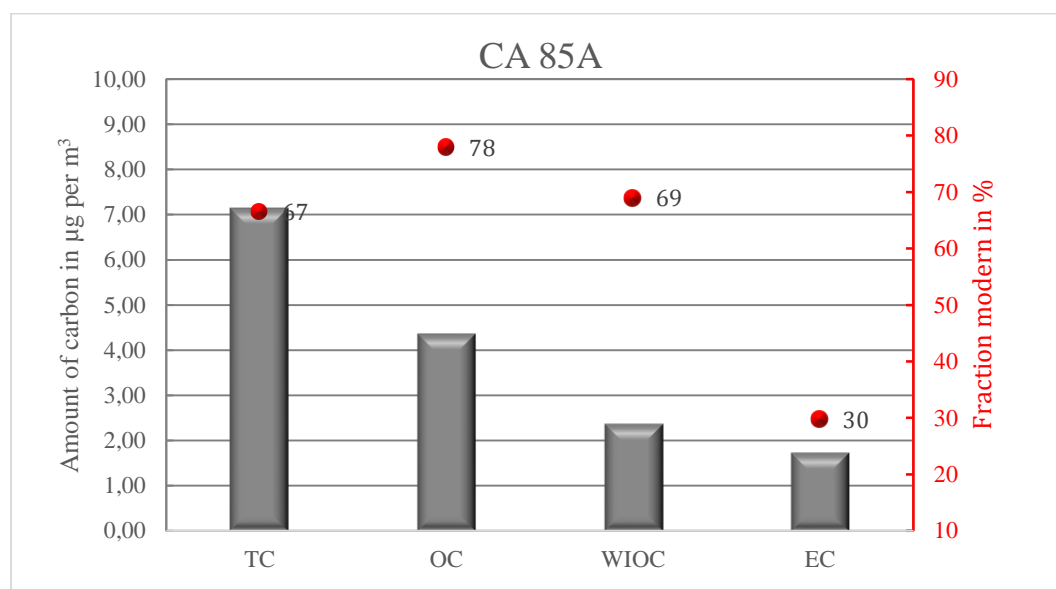


Figure 3.4, the amount of the different carbon fractions and fraction modern of sample CA 85A.

The total amount of carbon and of organic carbon were slightly lower compared with sample CA 84A. EC concentration was again lowest with only $1,74 \mu\text{g m}^{-3}$ followed by WIOC with $2,37 \mu\text{g m}^{-3}$ and OC was by far the most abundant fraction.

Most of the fractions had a slightly lower f_m compared with sample CA 84A except WIOC. OC had the highest f_m (78%) and EC had, with just 30 percent, the lowest fraction modern.

In figure 3.2 the trajectory of sample CA 85A is shown. At the beginning of the period the air mass had its origin in the Gulf of Genoa and went over France and Belgium. After two days the flow turned and the air mass originated from central Europe, South Germany and France and went over France, Germany, Luxemburg and the Ardennes towards the station.

During the period low pressure systems moved from the Atlantic towards Scandinavia and high pressure systems were present over France and (south)eastern Europe. At Cabauw there were periods with low clouds and fog and a little bit of sunshine, but no precipitation. The synoptic situation of November 19 is presented in figure 3.3.

From January 20 till January 23 2012 sample CA 99 was collected. As we can see in figure 3.5 the total amount of the different carbon fractions was (almost) a factor ten lower compared with CA 84A and CA 85A. OC was the most abundant fraction, but the difference with WIOC and EC was relatively bigger compared with samples CA 84A and CA 85A. Again EC was, with only 0,17 microgram per cubic meter, the smallest fraction.

The fraction modern of total carbon was roughly at the same level as the previous samples with 74 percent. The fraction modern of OC was not determined. But fraction modern of WIOC was much lower with 47 percent compared with CA 84A and CA 85A. The fraction modern of EC was with 24 percent lower than in samples CA 84A and CA 85A and was the lowest percentage of all fractions.

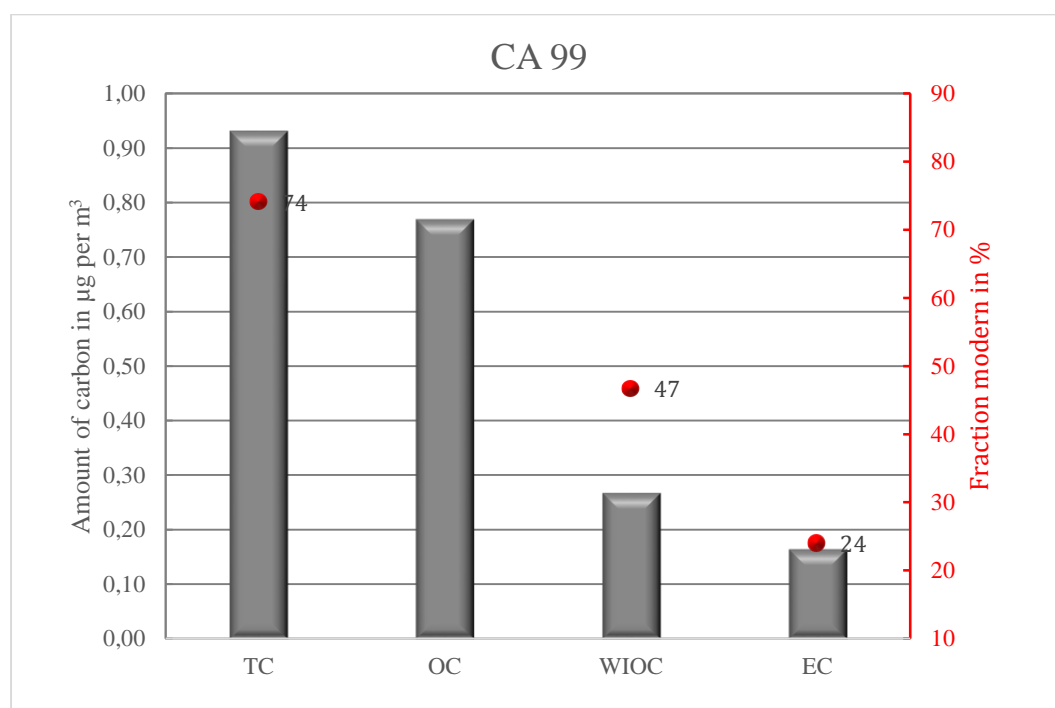


Figure 3.5, the amount of the different carbon fractions and fraction modern of sample CA 99. ^{14}C in OC was not determined.

In figure 3.2 the trajectory of sample CA 99 is shown. At the beginning of the period the air mass originated at the Atlantic ocean near Newfoundland and went over the Atlantic, Ireland, South England and the southern part of the Netherlands (perhaps passing the harbor of Rotterdam?) towards the station. On the last sampling day the air originated in an area above southern Greenland and went over northern Ireland, South England and the southern part of the Netherlands (perhaps passing the harbor of Rotterdam?) towards the station.

Between a high pressure system above the Azores and low pressure on the northern Atlantic a strong west circulation existed during the period. On the 20th there were some showers at Cabauw, during the night to the 21th a warm front passed. On the 21th a cold front passed.

During the 22th a low pressure system moved from the North sea to Denmark giving some precipitation and a lot of wind. On January 23 there were a lot of showers passing the station. For a synoptic overview of January 22 see figure 3.3

The results of sample CA 102 are presented in figure 3.6. The filters were collected from January 30 to February 2.

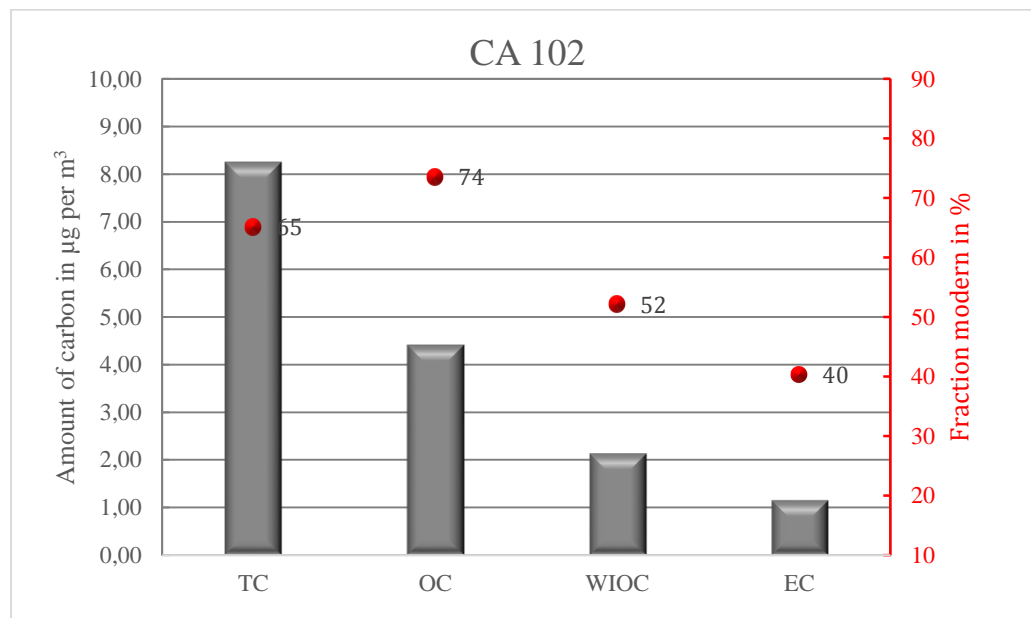


Figure 3.6, the amount of the different carbon fractions and fraction modern of sample CA 102.

In sample CA 102 the amount of the different carbon fractions was almost a factor ten higher compared with CA 99. Similar concentrations were found in sample CA 84A and CA 85A. EC was the least abundant fraction with 1,16 microgram per cubic meter.

In comparison with CA 99 the fraction modern of total carbon (65%) was lower but for WIOC (52%) and EC (40%) the fraction modern was higher.

According to the trajectory model, figure 3.2, air from Russia was blown over Belarus, northern Poland and northern Germany before it reached the high volume sampler. Later in the period the air mass went from Russia over Lithuania, Poland and northern Germany.

During the period a high pressure system over northern Russia dominated the weather at Cabauw. It remained dry and sunny with a strong easterly and later northeasterly wind. For an overview of the situation on January 31 2012 see figure 3.3.

The results of sample CA 106 are shown in figure 3.7. The filters were collected from February 13 to February 16 2012.

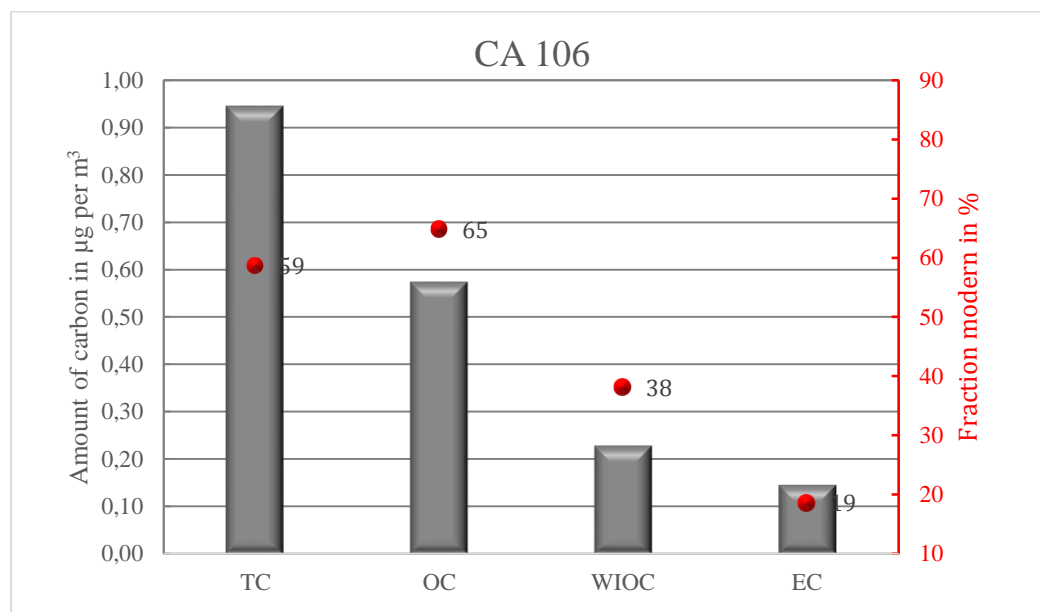


Figure 3.7, the amount of the different carbon fractions and fraction modern of sample CA 106.

The measured mass of the different carbon fractions was in the same order of magnitude as CA 99 and thus a factor ten smaller than CA 102. OC again was the most abundant fraction and EC had only a very small contribution with $0,15 \mu\text{g m}^{-3}$.

Of all the fall/winter samples CA 106 had the lowest percentage fraction modern with total carbon f_m of 59 percent. OC had the highest f_m (65%) followed by WIOC (38%) but EC with just 19 percent had the smallest fraction modern.

In figure 3.9 the trajectory is presented. The air went from an area south of Iceland over the Atlantic, the northern part of England and the North Sea towards the station. Only on February 14 the air mass went from the Atlantic to the north, near the coast of Iceland and went over the North Sea towards the Netherlands.

The station was on the east side of a high pressure system with its core west or southwest of Ireland. The wind was continuously northwest. An occlusion of a low, with its core over the Norwegian Sea, caused some rain on the evening of February 13. There were some showers on the fourteenth. The cold front of this system moved as a warm front on the evening of the fifteenth over the station with some showers. On the sixteenth it was cloudy but dry. An overview of the pressure systems at February 14 is presented in figure 3.3.

Sample CA 109 was collected from March 1 till March 7 and the results are presented in figure 3.8.

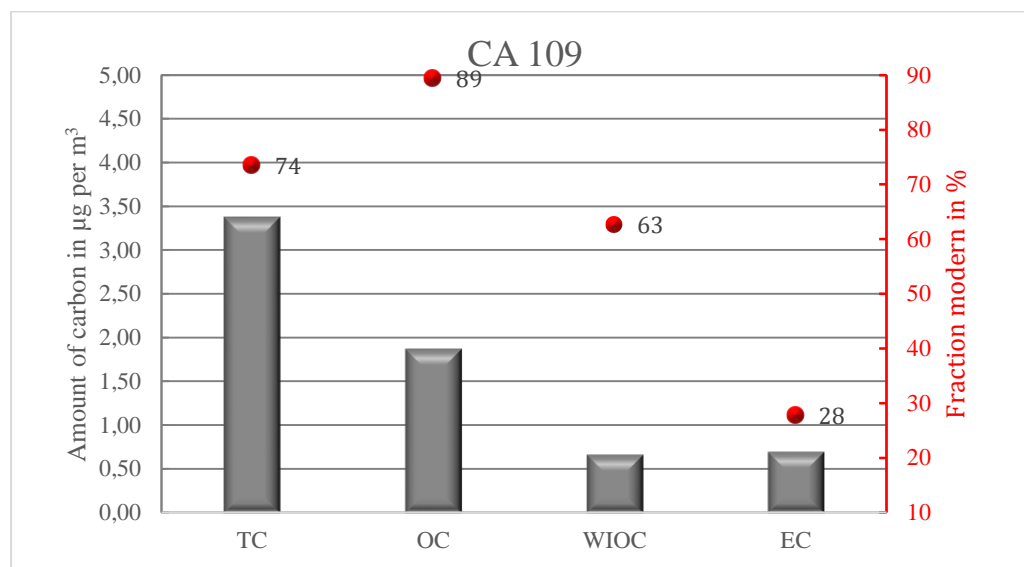


Figure 3.8, the amount of the different carbon fractions and fraction modern of sample CA 109.

With 3,37 microgram per cubic meter the concentration of total carbon was three times higher than CA 99 and CA 106 but also three times lower than CA 84A, CA 85A and CA 102. Again OC had the highest contribution. This was the only sample where WIOC ($0,67 \mu\text{gm}^{-3}$) had a slightly lower concentration than EC ($0,70 \mu\text{gm}^{-3}$).

For TC fraction modern was roughly at the same level as the other fall/winter samples but OC ($f_m = 89\%$) was much higher compared with the other samples. WIOC was with a fraction modern of 63% comparable with CA 84A and CA 85A. Yet again EC ($f_m = 28\%$) had the lowest fraction modern.

According to the trajectory model sample CA 109 had a continental and an Atlantic component, see figure 3.9. At the beginning of the period an air mass between France and England went over the Channel towards the Netherland making a curve above the Netherlands. After two days an air mass from east Germany went over France and Belgium towards the Netherlands. A day later an air mass from central France went over France and Belgium towards the station. Next day an air mass from the Atlantic went over Ireland, England, France and central Belgium. A day later an air mass from Ireland went over England, France, Luxemburg and east Belgium towards the station. On the last day the air mass had its origin in the Atlantic Ocean between Ireland and Iceland and went over England, France and central Belgium.

At the beginning of March a center of high pressure passed the station and went over the North Sea towards Scandinavia. During the 4th a center of low pressure moved from the Bay of Biscay towards our country and became stationary will slowly losing its activity on March 6. In the early morning of March 4 a cold front passed the station producing a lot of rain. On the 7th several fronts of a low pressure system near Iceland passed the station. For a synoptic overview see figure 3.3.

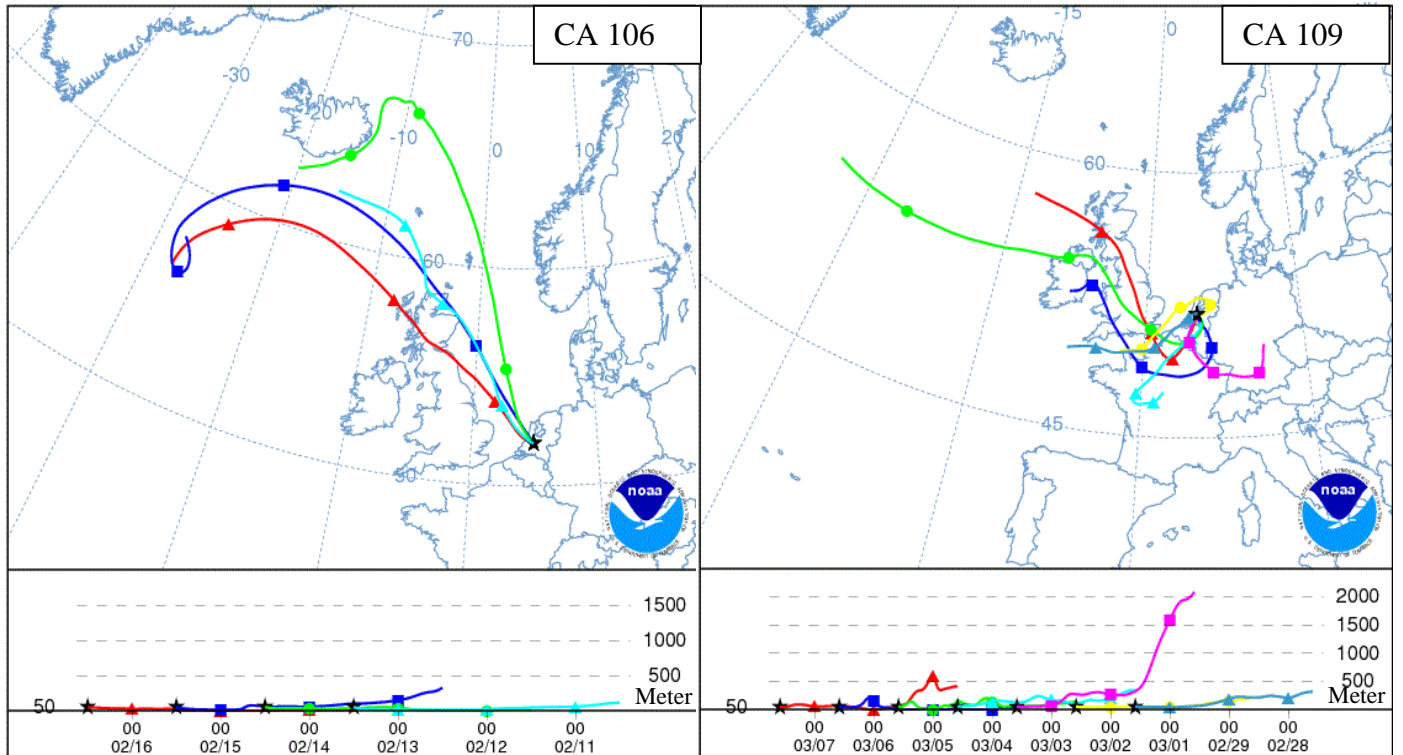


Figure 3.9, an overview of trajectories of samples CA 106 (February 13 till February 16 2012, left) and CA 109 (March 1 till March 7, right) source; <http://ready.arl.noaa.gov/HYSPLIT.php>, but modified.

3.2 Day and night filters

The results of CA 119A (night filter) and CA 120A (day filter) are presented in figure 3.10. The samples were collected from May 17 till May 20 2012.

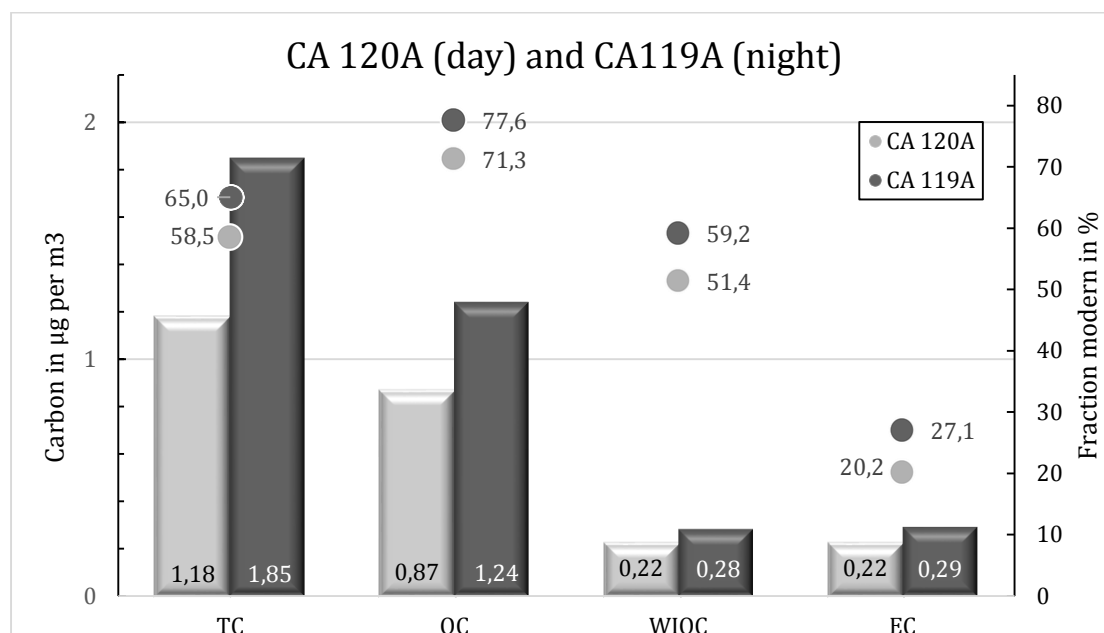


Figure 3.10, the amount of the different carbon fractions and fraction modern of sample CA 119A (night filter) and CA 120A (day filter). The dark grey bars and dots are for the night samples, the light grey bars and dots are for the day samples.

In figure 3.10 the bars indicate the concentration of the different carbon fractions (TC, OC, WIOC and EC) in microgram per cubic meter. The light grey bars show the results for the day filter and the dark grey bars show the results for the night filter and the units are displayed on the left y axis. For all the different carbon fractions the concentration of carbon in $\mu\text{g m}^{-3}$ was higher during the night period, with the smallest difference for EC and WIOC. There was no significant difference between EC and WIOC concentrations.

The dots in figure 3.10 show f_m of the corresponding carbon fractions. The light grey dots are for the day filter and the dark grey dots for the night filter. All different carbon fractions had at night higher fraction modern than during the day. Elemental carbon had a much lower fraction modern than WIOC and OC.

Figure 3.11 shows the air mass back trajectories for the sampling periods. In the first two days of the sampling period the air mass had its origin in the Atlantic Ocean north of Scotland and the Greenland Sea north of Iceland. It went over England, northern Belgium, central Germany and then back to the Netherlands. Later an air mass from southern France went over France and central Belgium towards the Netherlands. A day later an air mass from central Germany went over Luxemburg, eastern Netherlands, northern Netherlands before it went towards the station.

At the beginning of the period a high pressure center moved over the station towards Germany. After the 18th high pressure was building up over Scandinavia while low pressure systems were travelling from France to Germany and southeastern Europe.

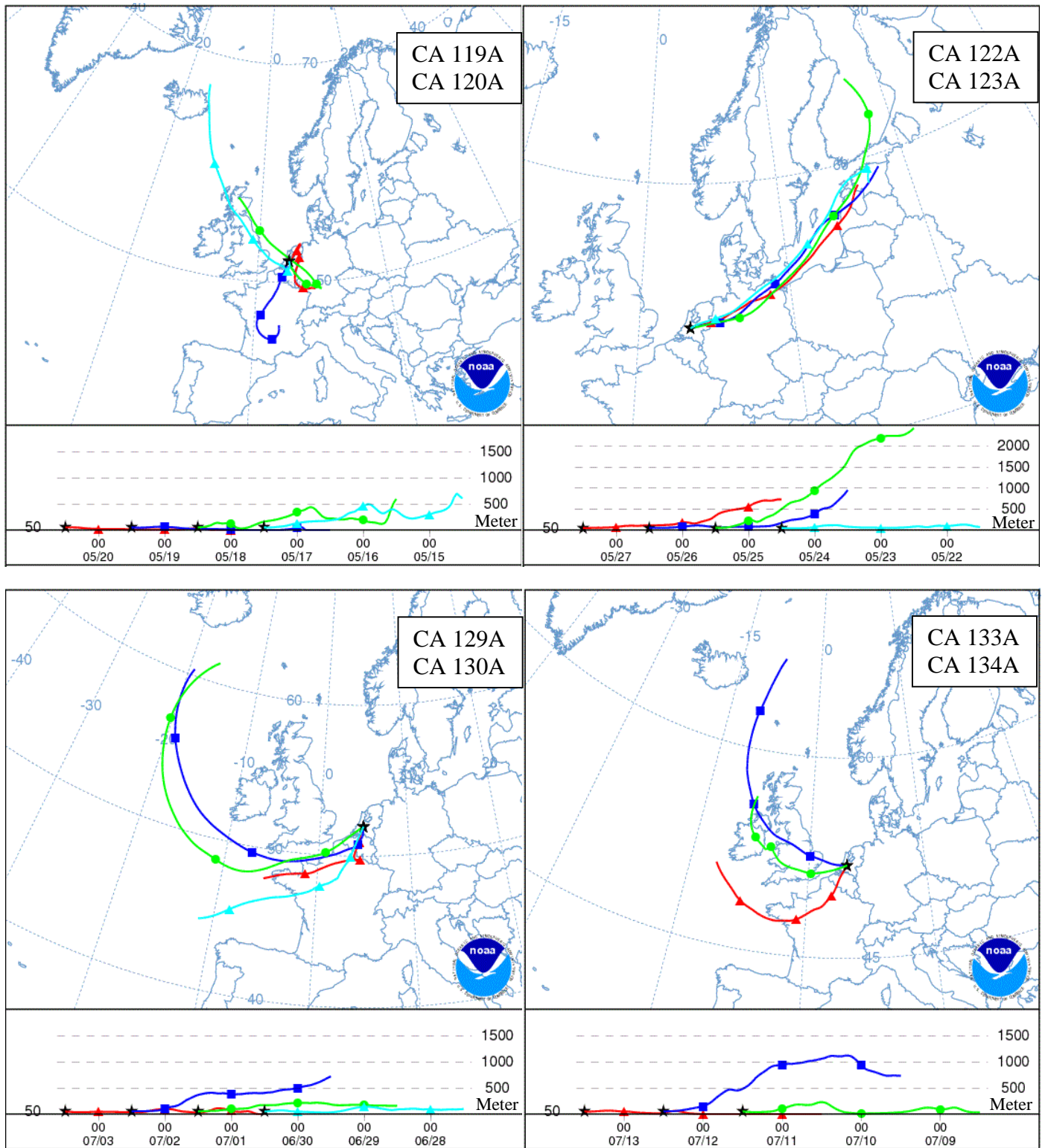


Figure 3.11, an overview of trajectories of samples CA 119A/120A (June 17 till June 20 2012, upper left), CA 122A/123A (June 24 till June 27 2012, upper right), CA 129A/130A (June 30 till July 3 2012 left) and CA 133A/134A (July 11 till July 13 2012, right), source; <http://ready.arl.noaa.gov/HYSPLIT.php> , modified.

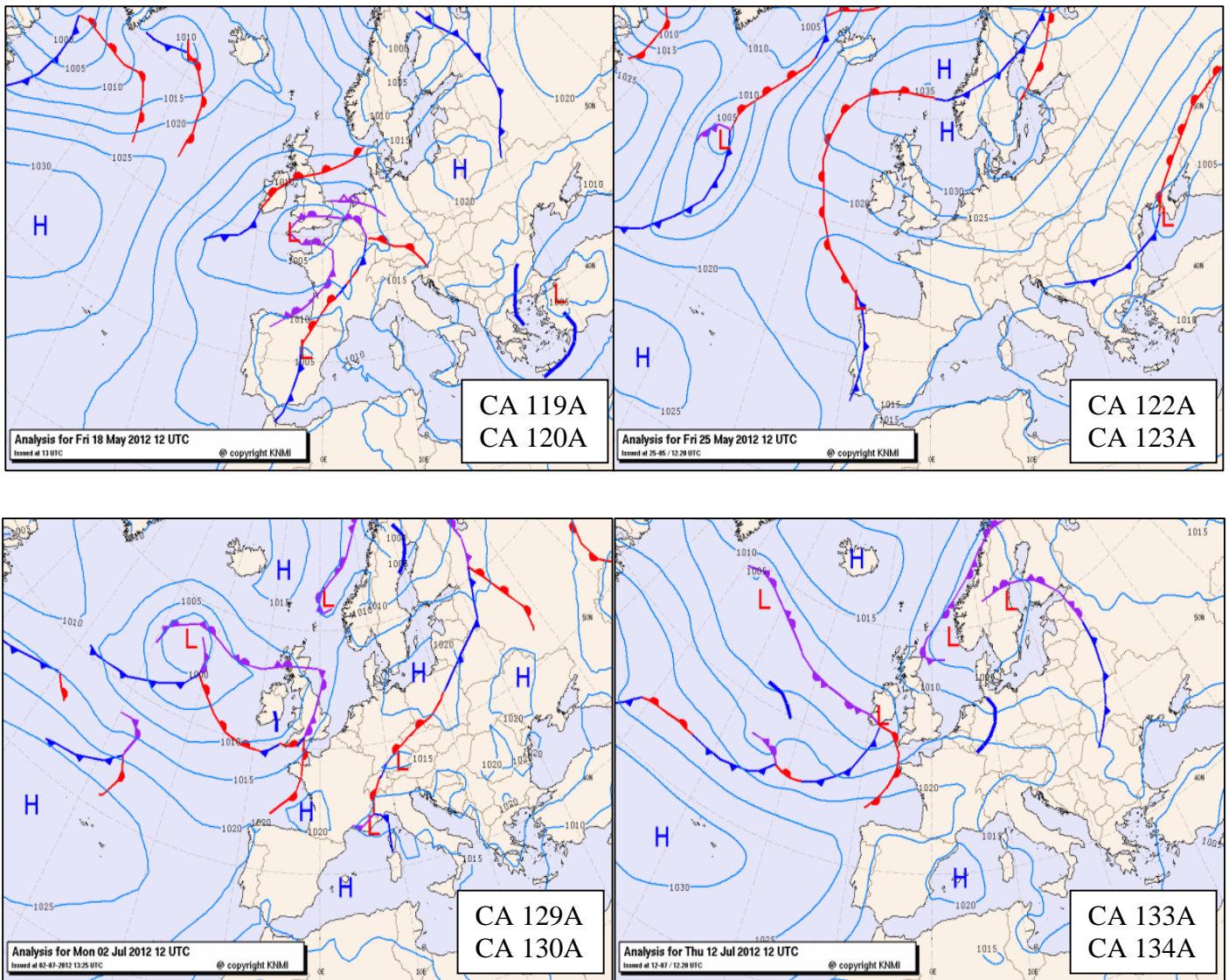


Figure 3.12, synoptic analyses of the different pressure systems and fronts during the different sampling periods. Source; KNMI, www.knmi.nl , modified.

A weak occluded front passed on May 18 with clouds and a few raindrops. During the night of May 19 a warm front passed the station. An overview of the synoptic situation on May 18 is presented in figure 3.12.

Samples CA 122A (day) and CA 123A (night) were collected from May 24 till May 27 and the results are presented in figure 3.13.

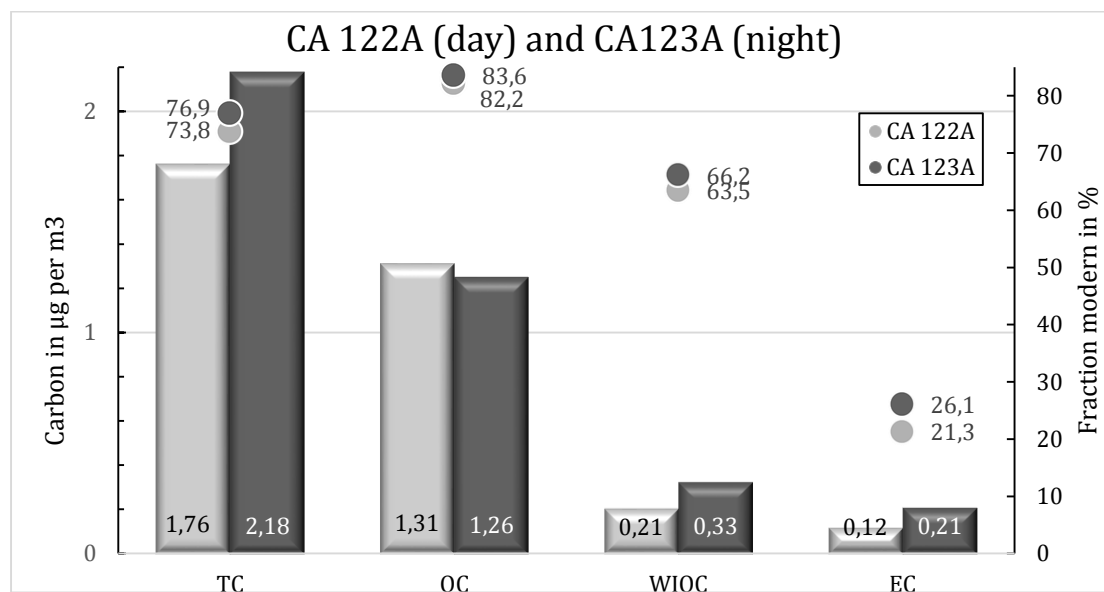


Figure 3.13, the amount of the different carbon fractions and fraction modern of sample CA 122A (day filter) and CA 123A (night filter).

Again the concentration of total carbon was higher during the night. This time slightly more ($2,18 \mu\text{gm}^{-3}$) than in sample CA 119A ($1,85 \mu\text{gm}^{-3}$). Organic carbon was less abundant during the night but there was more WIOC and EC making their share in total carbon bigger. Elemental carbon was the least abundant fraction found on the night and day samples.

During the night fraction modern was higher for all carbon fractions although the difference for organic carbon was rather small. Organic carbon had rather high values of fraction modern (83,3% and 82,2%) and so did WIOC but the share of modern particles in elemental carbon was rather low (26,1% and 21,3%).

In figure 3.11 the trajectory of the air mass during the sampling period is shown. It had its origin in Finland and northern Russia and was transported over Estonia, the Baltic Sea and northern Germany towards the station at Cabauw. This trajectory remained constant during the sampling period.

During this sampling period the weather was dominated by a high pressure system. Its center moved from south Scandinavia to the waters around Iceland. A secondary center was developing over the North Sea. The weather was quit dry and sunny. On May 27 some thunderstorms developed but it remained dry at the station. An overview of the pressure systems on May 25 is presented in figure 3.12.

Samples CA 129A (day) and CA 130A (night) were collected from June 30 till July 3, the results are presented in figure 3.14.

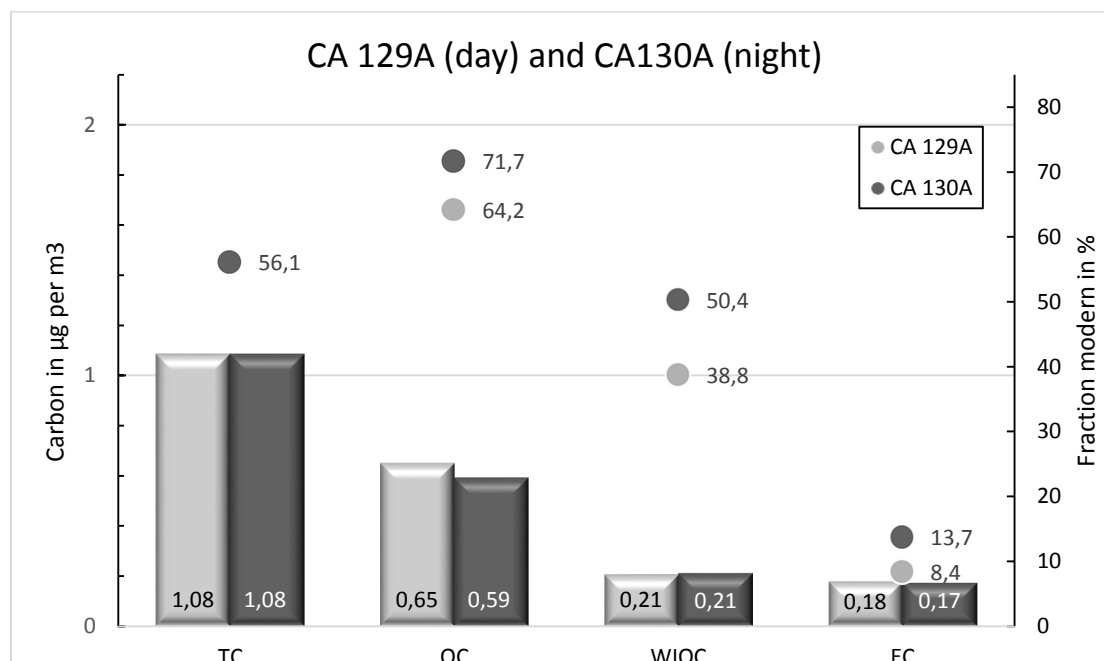


Figure 3.14, the amount of the different carbon fractions and fraction modern of sample CA 129A (day filter) and CA 130A (night filter).

The concentration of total carbon found during this period was much lower for both the day and night filter compared with the previous two periods. While the amount of WIOC and EC did not differ that much there was a lower concentration of organic carbon. Another difference with the previous two filter periods was that the concentration of all fractions throughout the day was constant.

The fraction modern of the different carbon fractions show a similar image as in the other sampling periods with lower values during daytime and higher values during nighttime. For EC f_m was extremely low during the night (13,7%) and during the day (8,4%).

At the beginning of the sampling period an air mass over the Atlantic, northwest of Portugal, went over the Gulf of Biscay, central France, central Belgium towards the station. The following two days an air mass on the Atlantic south of Iceland went south of England over the Channel and northwest France and western Belgium towards the Netherlands. After that an air mass went over northeast France and central Belgium towards the station. Details are presented in figure 3.11.

On June 30 a high pressure system lay over Eastern Europe. A shower gave some precipitation at the station (1mm). On the second of July a low pressure system near Britain started to influence the weather but it remained dry until the 3th of July. During that day some remnant thunderstorms from France passed the station. A synoptic overview of July 2 is presented in figure 3.12.

Samples CA 133A (day) and CA 134A (night) were collected from July 11 till July 13 and the results are presented in figure 3.15.

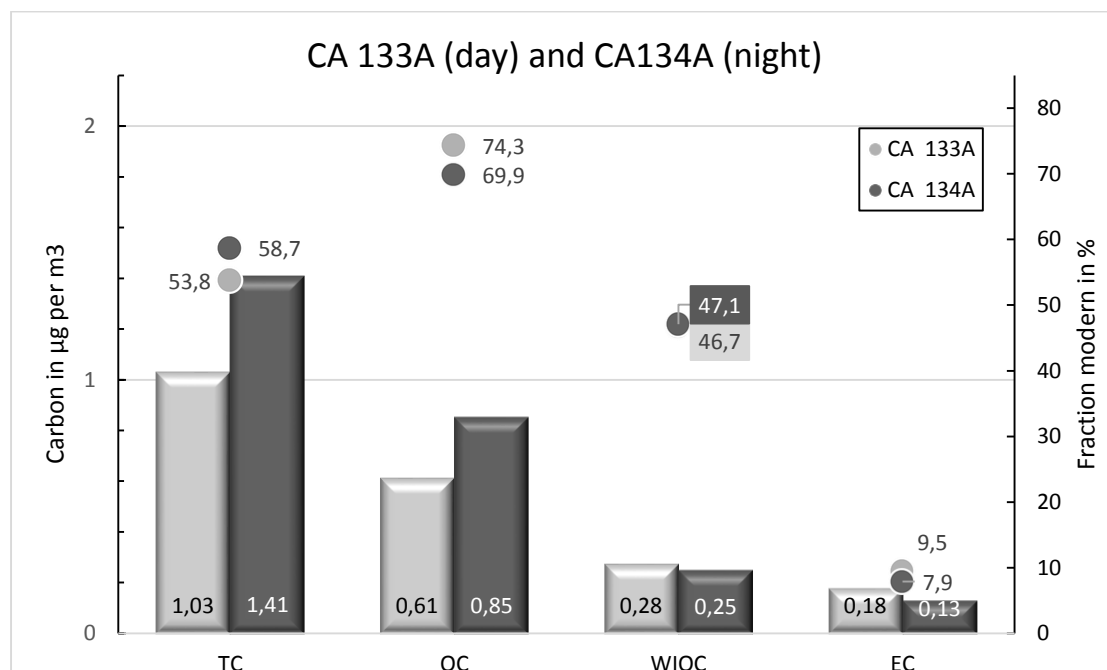


Figure 3.15, the amount of the different carbon fractions and fraction modern of sample CA 133A (day filter) and CA 134A (night filter).

Again there was more total carbon in the air during the night, this was due to a higher concentration of organic carbon. WIOC and EC concentrations were higher during the day. But throughout the period (day and night) EC concentration was lowest and with $0,18 \mu\text{gm}^{-3}$ and $0,13 \mu\text{gm}^{-3}$ it was among the lowest values measured in this thesis.

For total carbon the fraction modern was higher during the night but for organic carbon and elemental carbon the highest values were measured during the day. For WIOC the anomaly was very small. The f_m values of elemental carbon (9,5% during the day and 7,9% during the night) were the lowest of all fractions and also the lowest of all samples in this thesis, in fact it was nearly fossil.

At the beginning of the period an air mass went from the Atlantic, between England and Iceland, over northern Ireland and England towards the Netherlands. At the end of the period air from the Atlantic, west of Ireland, went over northwest France and western Belgium towards the station. Details are presented in figure 3.11.

During the period low pressure between Britain and Scandinavia dominated the weather. Everyday showers produced precipitation (approximately 4 millimeter a day) at the station. And on July 13 a warm front and a cold front passed the station. A map with the pressure systems and fronts on July 12 is presented in figure 3.12.

4. Discussion

From the results of chapter three some very interesting patterns emerge. These will be discussed in this chapter. In paragraph 4.1 the results of the fall/winter samples are subject of discussion followed by the day and night samples in paragraph 4.2.

4.1 Fall/winter samples

Elemental carbon has the lowest concentration and also the lowest f_m of all fractions at Cabauw. Water insoluble organic carbon of sample CA 109 has a lower concentration. But with $0,03 \mu\text{gm}^{-3}$ this difference is very small and not significant.

In figure 4.1 an overview of the collected fall/winter samples is presented. In blue the values of the Atlantic air masses are shown and in yellow the continental air masses. For the “Atlantic” sample CA 99 the f_m of OC is unknown and therefore its value is absent in figure 4.1. For CA 99 the f_m of OC should be around 90 percent when f_m of TC, WIOC and EC are taken into account.

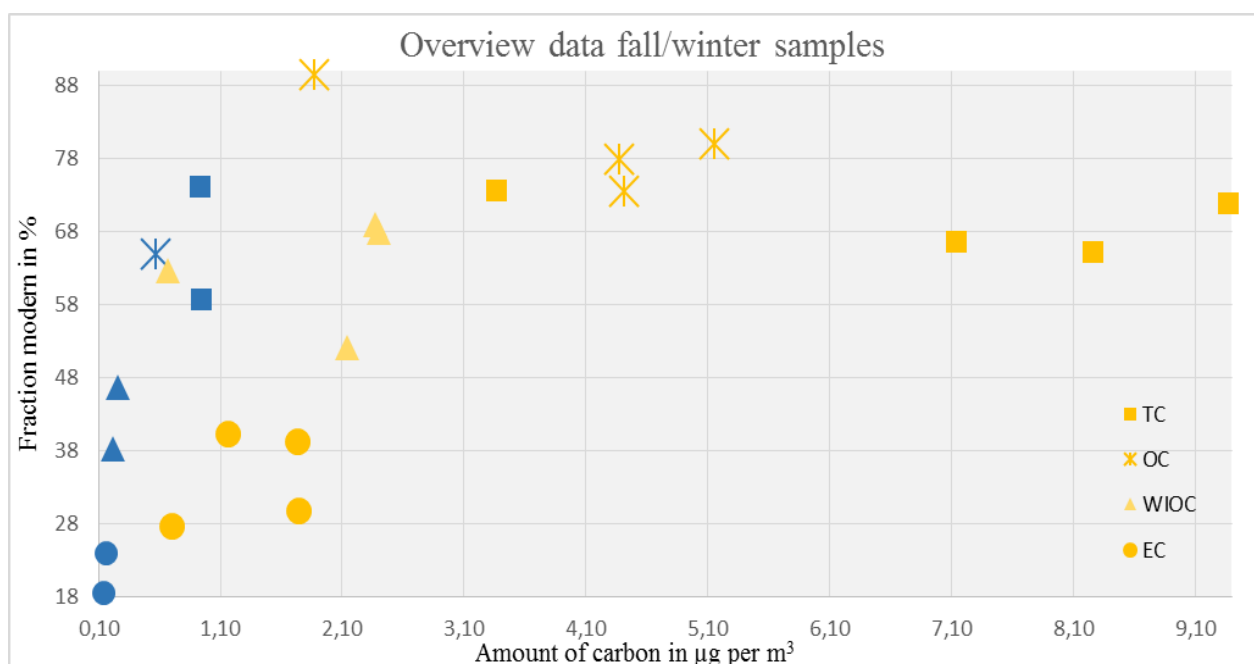


Figure 4.1, presentation of the fall/winter sample data. In blue “Atlantic” air masses and in yellow continental air masses.

The TC concentration ranged from $0,93 \mu\text{gm}^{-3}$ till $9,37 \mu\text{gm}^{-3}$, OC from $0,57 \mu\text{gm}^{-3}$ till $5,15 \mu\text{gm}^{-3}$, WIOC from $0,23 \mu\text{gm}^{-3}$ till $2,40 \mu\text{gm}^{-3}$ and EC from $0,15 \mu\text{gm}^{-3}$ till $1,74 \mu\text{gm}^{-3}$. The fraction modern of TC ranged from 59% till 74%, OC from 65% till 89%, WIOC from 38% till 69% and EC from 19% till 40%.

It is interesting to compare the results with the measurements done by Szidat (2007), in Switzerland, because both sampling campaigns were during wintertime. In comparison with Roveredo and Moleno (two small Swiss villages) the EC concentration is much lower at Cabauw. The difference is almost a factor ten and

peaks of $9,5 \mu\text{gm}^{-3}$ were measured at Moleno. Cabauw, Roveredo and Moleno have similar values for the ratio of EC over TC ranging from 0,14 till 0,24. An explanation for the significant higher concentrations of the different carbon fractions is the appearance of much stronger winter-time inversions in the Alpine valleys, sometimes only several tens of meters high. Only during nighttime such inversions were found at Cabauw, see table 4.2. Another interesting fact is the difference in fraction modern between the three sites. Overall, the fraction modern of EC is much higher in the Alpine valleys with peaks reaching 90 percent. In EC, modern carbon comes from wood burning, and fossil carbon mainly from traffic. At Cabauw more fossil carbon is found. Residential wood burning is less important at Cabauw, in comparison with the Alps.

As shown in figure 4.1, continental air masses have a much higher concentration of the different carbon fractions compared to Atlantic air masses at Cabauw. This is simply due to the fact that there are much more anthropogenic and non-anthropogenic sources of aerosol carbon on the continent. In comparison with measurements done in southern Sweden (Genberg et al., 2011) the concentration of OC and EC are slightly higher at Cabauw.

One might argue that meteorological conditions also played a role in the concentration of the different carbon fractions. During the continental phase the air masses were relatively dry, resulting in dry and sunny weather most of the time. This is ideal for the formation of secondary aerosols. While during an Atlantic period the air is moist and there are clouds and precipitation. As mentioned in chapter one particles in the accumulation mode can either serve as cloud condensation nuclei and be washed out by precipitation (in-cloud scavenging) or they can be scavenged by precipitation below the cloud. Such processes occur more frequently during an Atlantic period. But for particles in the nucleation and coarse mode these meteorological circumstances are less relevant. It remains unclear how big the role of precipitation versus air mass origin was in causing the low concentrations in marine air masses. More research is recommended.

Elemental carbon and WIOC have much lower values of f_m during an “Atlantic” period in comparison with a “continental” period. For TC and OC there does not seem to be a strong difference.

In figure 4.2 the concentration of the different fractions and f_m of continental and Atlantic air masses are compared. In this figure the Atlantic sector consists of samples CA 99 and CA 106. The continental sector is composed of CA 84A, CA 85A and CA 102. For each sector the average of the different carbon fractions has been taken. It should be noted that for CA 99 the fraction modern of OC was not available. Therefore f_m of the different fractions are not in proportion with total carbon in the Atlantic sector.

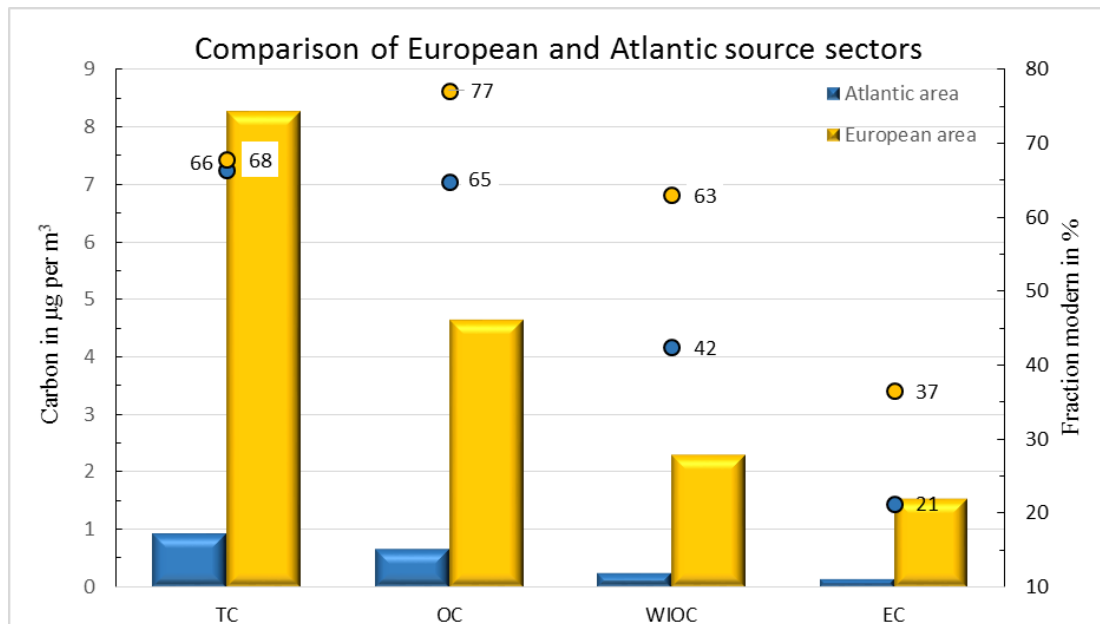


Figure 4.2, a comparison of carbon concentration and fraction modern in “Atlantic” and “European” air masses.

From figure 4.2 it is very obvious that the highest concentrations and fraction modern are found in air masses from the continental sector.

An important biogenic source in the ocean is plankton activity and an important anthropogenic source are vessels combusting cheap oil. Because the campaign period went from November till March the contribution of plankton is rather low. One could conclude from figure 4.2 that there are less carbon sources in the Atlantic sector and they are mainly anthropogenic.

But this conclusion is not as straightforward as it seems. Ceburnis et al. (2011) conducted an air quality campaign on vessels in the Atlantic Ocean and at Mace Head, an isolated place in western Ireland. Total carbon concentrations in clean marine samples ranged from $0,07 \mu\text{g m}^{-3}$ till $0,35 \mu\text{g m}^{-3}$, a factor ten lower compared with Cabauw. The fraction modern of TC (approximately 80%) and OC (approximately 90%) of these clean marine samples are slightly higher than the samples from Cabauw. So there is a lot of pollution before the Atlantic air mass reaches Cabauw if the results from this paper are representative for the marine background of the Cabauw filters. Most ships are found near the coastline and in the Channel, enriching the air with fossil carbons. For some samples the trajectory went over the Channel and they always crossed coastlines. Most trajectories also passed big harbors like Antwerp and Rotterdam where a lot of industrial activities occur. One must conclude that the biggest contribution of carbon, mainly fossil, on “Atlantic” aerosols is in the last hundred kilometer before the air mass reaches Cabauw. But notwithstanding these findings the “Atlantic” air mass measured at Cabauw has lower concentrations of the different carbon species and lower fraction modern than the “continental” air mass collected at Cabauw. The amount of samples collected is limited and therefore more research is recommended to obtain more certainty.

4.2 Day and night samples

Again elemental carbon has the lowest concentration of all fractions. This is true for all filters. The fraction modern of EC is also lower during daytime than during nighttime. Much of the elemental carbon originates from fossil fuel burning and this indicates a relative increase of fossil sources during the day.

The total carbon concentration is in three of four cases higher during the night. Sometimes it is due to a high concentration of OC (CA 133A/CA 134A) or to a high concentration of WIOC and EC (CA 122A/CA 123A) and sometimes all fractions are more abundant during the night (CA 119A/CA 120A). Only sample CA 129A/CA 130A shows no significant diurnal cycle.

A possible explanation for the higher concentrations during the night is the appearance of an inversion layer at lower levels in the atmosphere. Indeed a low inversion layer is observed during the night, see table 4.3. It should be noted that the appearance of an inversion layer does not mean that mixing could not occur. When a low pressure system or fronts approach Cabauw a forced lifting mechanism could enhance mixing.

Another explanation of the higher nighttime concentrations is the condensation of semi volatile carbon due to cooling of the atmosphere during the night. As a result carbon concentration increases during the night. This process does not play a role for elemental carbon but is important for OC and WIOC concentrations. This might explain the higher values of OC seen in samples CA 119A/CA 120A and CA 133A/CA 134A. Semi volatile carbon has both biogenic and anthropogenic sources. During summertime there are more biogenic sources. Therefore the condensation of semi volatile carbon most likely contributes to higher f_m during the night for OC and WIOC.

The formation of secondary aerosols on sunny days contributes to the organic carbon concentration during daytime and higher f_m . The weather was dry and sunny during CA 122A/CA 123A and this might explain the higher concentration of OC during daytime. Sample CA 129A/CA 130A also shows a higher concentration of OC during the day but at the beginning of the sampling period and at the end it was a bit cloudy. In both sampling periods the difference in OC concentration between day and night is rather small. Secondary aerosol formation together with an increase in traffic emissions, could be high enough to overcome an increase in OC concentrations during the night, despite dilution due to the higher boundary layer.

The fraction modern of the different carbon fractions is also higher during the night. During daytime there is more traffic, resulting in more fossil carbons and therefore f_m is lower between 7:00 and 19:00. Only CA 133A/CA 134A shows a different pattern, with high f_m of OC during the day.

Sample CA 133A/CA 134A is the only midweek day/night sample. During a midweek there is more (commuting) traffic between 7:00 and 19:00. This might explain the higher concentrations of EC and WIOC during daytime.

The trajectories also play an important role in the concentration and f_m of the different carbon fractions. During CA 122A/CA 123A the air mass had a “continental” origin while CA 129A/CA 130A and CA 133A/CA 134A were collected in “Atlantic” air masses. As with the fall/winter samples the lowest concentrations and f_m are found in these “Atlantic” air masses.

In summary, inversion layers and the condensation of semi volatile organic carbon contribute to the concentration of the different carbon fractions during the night. Commuting traffic and the formation of secondary aerosols contribute to the concentration of the different carbon fractions during the day. But the trajectory always play an important role in the concentration and f_m of the different carbon fractions throughout the day.

When comparing the ratio of WIOC and OC another interesting feature can be found, as presented in table 4.1.

sample code	date start	date end	WIOC/OC	fm OC (%)	fm WIOC (%)
CA 84A	14-Nov-2011 11:30	17-Nov-2011 15:30	0,47	80	67,9
CA 85A	17-Nov-2011 15:30	21-Nov-2011 18:00	0,54	78	69,0
CA 99	20-Jan-2012 18:05	23-Jan-2012 15:50	0,35	Not Available	46,7
CA 102	30-Jan-2012 19:50	3-Feb-2012 14:00	0,48	74	52,2
CA 106	13-Feb-2012 12:05	16-Feb-2012 17:00	0,40	65	38,2
CA 109	1-Mar-2012 12:35	7-Mar-2012 18:45	0,36	89	62,7
Average			0,43	77,2	56,1

sample code	date start	date end	WIOC/OC	fm OC (%)	fm WIOC (%)
CA 119A	17-May-2012 19:00	20-May-2012 07:00	0,23	77,6	59,2
CA 120A	18-May-2012 07:00	20-May-2012 12:00	0,26	71,3	51,4
CA 122A	25-May-2012 07:22	27-May-2012 19:22	0,16	82,2	63,5
CA 123A	24-May-2012 19:22	27-May-2012 07:22	0,26	83,6	66,2
CA 129A	1-Jul-2012 07:00	3-Jul-2012 19:00	0,32	64,2	38,8
CA 130A	30-Jun-2012 19:00	3-Jul-2012 07:00	0,36	71,7	50,4
CA 133A	12-Jul-2012 07:00	13-Jul-2012 19:00	0,45	74,3	46,7
CA 134A	11-Jul-2012 19:00	13-Jul-2012 07:00	0,30	68,1	47,1
Average			0,29	74,1	52,9

Table 4.1, the ratio of WIOC over OC of the different samples and their fraction modern. Blue for Atlantic and yellow for continental air masses.

If the different sample types were considered separately the WIOC/OC ratio seems rather constant. Combined the average of this ratio is approximately 1/3 but the day/night samples have a much lower ratio compared with the fall/winter samples. The fall/winter samples were collected during autumn/winter and the day/night filters during spring/summer. There seems to be a seasonal cycle. This cycle can be explained by a seasonal change of carbon sources. The f_m of WIOC is on average lower during the summer although the difference is rather small. During spring and summer the formation of secondary aerosols is an important process. Most of these secondary aerosols are water soluble organic carbon. This process explains the difference in WIOC over OC ratio between summer and wintertime.

CA 84A	14-11-2011	15-11-2011	16-11-2011	17-11-2011			
Maximum Temperature in °C	8,4	5,9	7,3	8			
Minimum Temperature in °C	1,4	-1,7	-0,7	-0,8			
Winddirection at 10m in °	100))60	60))80	80))140	130)170			
Windspeed in km/h	11	10)16)11	14))6	6)14)9			
Relative Humidity %	99)77)96	99)78)93	93)69)96	99)94)97			
Stable or Convective Day/Night	CON/ST	CON/ST	ST/ST	ST/ST			
Mixed Height Day/Night in m	210/0	170/0	0/0	0/0			
Lowest Inversion Layer D/N in m	210/25	170/25	180/25	170/25			
CA 85	17-11-2011	18-11-2011	19-11-2011	20-11-2011	21-11-2011		
Stable or Convective Day/Night	ST/ST	ST/ST	ST/ST	ST/ST	ST/ST		
Mixed Height Day/Night in m	0/0	0/0	0/0	0/0	0/0		
Lowest Inversion Layer D/N in m	100/50	100/50	100/50	75/50	50/50		
Maximum Temperature in °C	8	9,9	10,5	4,4	3		
Minimum Temperature in °C	-0,8	2,7	-0,7	-1,3	0,2		
Winddirection at 10m in °	150)) 200	170)190)120	110	90))10	40)) 90		
Windspeed in km/h	8)14)6	8)16)4	4)10)2	3)) 5	5		
Relative Humidity %	99)94)97	99)90)99	100)81)100	99	99		
CA 99	20-01-2012	21-01-2012	22-01-2012	23-01-2012			
Maximum Temperature in °C	6,6	10,6	9,8	7,1			
Minimum Temperature in °C	0,9	1,4	4,6	1,9			
Winddirection at 10m in °	280))220	210))290	280	270			
Windspeed in km/h	33))12	12))44	40)52)16	16)28)16			
Relative Humidity %	87)71)96	99)68)72	68)69)92	94)76)92			
Stable or Convective Day/Night	ST/ST	ST/ST	ST/ST	ST/ST			
Mixed Height Day/Night in m	0/0	0/0	0/0	0/0			
Lowest Inversion Layer D/N in m	600/75	1400/1400	1400/25	800/25			
CA 102	30-1-2012	31-1-2012	1-2-2012	2-2-2012			
Maximum Temperature in °C	-0,9	-0,9	-1,2	-3,1			
Minimum Temperature in °C	-2,1	-5,5	-7,6	-8,5			
Winddirection at 10m in °	35)4:30)80	65	60))50	50			
Windspeed in km/h	9))12	12))22	20)30)20	20))13			
Relative Humidity %	95)85)96	84)60)74	78)36)52	68)32)67			
Stable or Convective Day/Night	ST/ST	ST/ST	ST/ST	ST/ST			
Mixed Height Day/Night in m	0/0	0/0	0/0	0/0			
Lowest Inversion Layer D/N in m	250/200	250/210	300/25	300/50			
CA 106	13-02-2012	14-02-2012	15-02-2012	16-02-2012			
Maximum Temperature in °C	4,5	5,9	6,6	7,5			
Minimum Temperature in °C	-1,2	2	4,4	2,4			
Winddirection at 10m in °	230))320	340))290	300	310))230			
Windspeed in km/h	9))15	16))26	30))12	12))18			
Relative Humidity %	99)85)99	99)81)98	98)79)98	99)88)99			
Stable or Convective Day/Night	ST/ST	CON/ST	CON/ST	ST/ST			
Mixed Height Day/Night in m	0/0	1450/0	1450/0	0/0			
Lowest Inversion Layer D/N in m	1400/25	1450/25	1450/25	200/25			
CA 109	1-3-2012	2-3-2012	3-3-2012	4-3-2012	5-3-2012	6-3-2012	7-3-2012
Maximum Temperature in °C	10	11.3	12.3	10.8	8.7	9.7	6.4
Minimum Temperature in °C	8.3	6.8	6.6	4.4	3.7	1.5	0.6
Winddirection at 10m in °	210))330	360))90	90))200	200))120	120))100	90))210	190))310
Windspeed in km/h	6	6))11)9	11)16)12	14	14)24)14	12))6))18))8	8))36))21
Relative Humidity %	99)92)99	99)75)94	98)77)95	99)77)99	98)74)84	90)59)99	99)77)98)87
Stable or Convective Day/Night	ST/ST	CON/ST	ST/ST	ST/ST	CON/ST	CON/ST	ST/ST
Mixed Height Day/Night in m	0/0	860/0	0/0	0/0	1000/0	1500/0	0/0
Lowest Inversion Layer D/N in m	500/500	860/25	1450/25	200/50	1000/1000	1500/25	700/25

Table 4.2, overview of meteorological data collected during the fall/winter campaign. The temperature, wind direction, wind speed and relative humidity are from the KNMI weather station at Cabauw. Information about convection, mixed height and lowest inversion layer are from the balloon soundings at De Bilt at 00:00 and 12:00 Zulu time. The) is used to show a gradual change in the value of the parameter. CON stands for convective and ST for stable.

CA 119A, CA 120A	17 mei 2012	18 mei 2012	19 mei 2012	20 mei 2012
Maximum Temperature in °C	15.1	19.0	20	21.4
Minimum Temperature in °C	3.1	9.6	11.1	11.3
Winddirection at 10m in °	200)70	80)180	140)360	360
Windspeed in km/h	8)15	15)24)19	8)18)12	12)16)12
Relative Humidity %	100)41)65	72)57)98	99)48)87	98)71)96
Stable or Convective Day/Night	CON/ST	CON/ST	CON/ST	CON/ST
Mixed Height Day/Night in m	2000/0	700/0	2200/0	500/0
Lowest Inversion Layer D/N in m	1800/100	700/25	2200/25	300/25
CA 122A, CA 123A	24 mei 2012	25 mei 2012	26 mei 2012	27 mei 2012
Maximum Temperature in °C	27.7	25.3	24.8	26.3
Minimum Temperature in °C	16.3	15.5	14.9	14.7
Winddirection at 10m in °	20)80	75)100)45	45)110)70	70)10
Windspeed in km/h	4)13	11)30)14	14)22)12	9)20)6
Relative Humidity %	100)46)50	57)34)74	84)31)50	77)35)84
Stable or Convective Day/Night	CON/ST	CON/ST	CON/ST	CON/ST
Mixed Height Day/Night in m	900/0	1500/0	1400/0	5000/0
Lowest Inversion Layer D/N in m	850/25	1100/50	1400/25	1800/25
CA 129A, CA 130A	30 juni 2012	1 juli 2012	2 juli 2012	3 juli 2012
Maximum Temperature in °C	23.9	18.5	22	24
Minimum Temperature in °C	14.6	11.1	10.6	14.4
Winddirection at 10m in °	190)200	220)250)220	230)120	130)240)30
Windspeed in km/h	9)30)10	12)28)12	12)16)10	12)18)6
Relative Humidity %	97)52)98	94)58)93	94)47)74	88)57)93
Stable or Convective Day/Night	CON/ST	CON/ST	CON/ST	CON/ST
Mixed Height Day/Night in m	3500/0	3400/0	2000/0	3500/0
Lowest Inversion Layer D/N in m	1500/25	2800/25	1600/25	1500/25
CA 133A, CA 134A	11 juli 2012	12 juli 2012	13 juli 2012	
Maximum Temperature in °C	19.1	18.2	20.5	
Minimum Temperature in °C	14.1	11.5	13	
Winddirection at 10m in °	200)230	220)20	20)220	
Windspeed in km/h	14)30)24	21)30)6	6)25)12	
Relative Humidity %	94)55)88	97)51)87	99)61)88	
Stable or Convective Day/Night	CON/ST	CON/ST	CON/ST	
Mixed Height Day/Night in m	3000/0	3500/0	3000/0	
Lowest Inversion Layer D/N in m	2400/50	2000/25	3000/50	

Table 4.3, overview of meteorological data collected during the day/night filters campaign. The temperature, wind direction, wind speed and relative humidity are from the KNMI weather station at Cabauw. Information about convection, mixed height and lowest inversion layer are from the balloon soundings at De Bilt at 00:00 and 12:00 Zulu time. The) is used to show a gradual change in the value of the parameter. CON stands for convective and ST for stable.

5. Conclusions

From the discussion in chapter 4 several conclusions emerge.

5.1 Fall/winter samples

The carbon concentration of continental air masses is much higher than the carbon concentration of Atlantic air masses. The difference in concentration between an “Atlantic” period and a “continental” period is almost a factor ten at Cabauw. The f_m of WIOC and EC are much lower during an “Atlantic” period in comparison with a “continental” period. The biggest contribution of carbon, mainly fossil, on “Atlantic” aerosols is in the last hundred kilometer before the air mass reaches Cabauw, if the results from this paper are representative for the marine background of the Cabauw filters. Elemental carbon has the lowest concentration and the lowest f_m of all fractions. The main source of EC is fossil fuel burning and only a small part is from biomass burning.

5.2 Day and night samples

Again elemental carbon has the lowest concentration and the lowest f_m of all fractions throughout the day. The total carbon concentration is in three of four cases higher during the night. And f_m of the different fractions is in three of four cases lower during the day.

Inversion layers and the condensation of semi volatile organic carbons contribute to higher concentrations of the different carbon fractions during the night. The condensation of biogenic semi volatile organic carbons leads to higher f_m of OC and WIOC during the night. Inversion layers do not influence f_m directly. Commuting traffic and the formation of secondary aerosols play an important role in the concentration of the different carbon fractions during the day. Traffic contributes to lower f_m while the formation of secondary aerosols contributes to higher f_m during the day. But the air mass origin always plays an important role in the concentration and f_m of the different carbon fractions throughout the day. This highlights the dominant influence of long range transport versus the more regional sources that cause the diurnal variations.

There seems to be a seasonal cycle in the ratio of WIOC over OC. This cycle can be explained by the formation of secondary aerosols during spring and summer, that are primarily water soluble. It should be noted that the amount of samples is limited and therefore more research is recommended to obtain more certainty about the conclusions made in this chapter.

6. References

D. Ceburnis, A. Garbaras, S. Szidat, M. Rinaldi, S. Fahrni, N. Perron, L. Wacker, S. Leinert, V. Remeikis, M. C. Facchini, A. S. H. Prevot, S. G. Jennings, M. Ramonet, C. D. O'Dowd, (2011). Quantification of the carbonaceous matter origin in submicron marine aerosol by ^{13}C and ^{14}C isotope analysis, *Atmos. Chem. Phys.*, 11, 8593–8606, www.atmos-chem-phys.net/11/8593/2011/, doi:10.5194/acp-11-8593-2011.

Currie, L.A., (2000). Evolution and Multidisciplinary Frontiers of ^{14}C Aerosol Science, *Radiocarbon*, vol 42, nr 1, 2000, p 115–126.

U. Dusek, H.M. ten Brink, H.A.J. Meijer, G. Kos, D. Mrozek, T. Röckmann, R. Holzinger, E.P. Weijers, (2013). The contribution of fossil sources to the organic aerosol in the Netherlands, *Atmospheric Environment* 74, p 169-176, <http://dx.doi.org/10.1016/j.atmosenv.2013.03.015>.

Dusek, U., Monaco, M., Kappetijn, A., Meijer, H. A. J., Szidat, S., Röckmann, T., (2013). The fossil fraction of carbon in PM_{2.5}: Variations on seasonal and diurnal time scales.

Dusek, U., Monaco, M., Kappetijn, A., Meijer, H. A. J., van der Plicht, J., Szidat, S., Röckmann, T., (2013). Fossil and modern sources of aerosol carbon in the Netherlands – A year-long radiocarbon study.

S. Fuzzi, M. O. Andreae, B. J. Huebert, M. Kulmala, T. C. Bond, M. Boy, S. J. Doherty, A. Guenther, M. Kanakidou, K. Kawamura, V.-M. Kerminen, U. Lohmann, L. M. Russell, and U. Pöschl, (2006). Critical assessment of the current state of scientific knowledge, terminology, and research needs concerning the role of organic aerosols in the atmosphere, climate, and global change, *Atmos. Chem. Phys.*, 6, 2017–2038.

A. Gelencsér, B. May, D. Simpson, A. Sánchez-Ochoa, A. Kasper-Giebl, H. Puxbaum, A. Caseiro, C. Pio, M. Legrand, (2007). Source apportionment of PM_{2.5} organic aerosol over Europe: Primary/secondary, natural/anthropogenic, and fossil/biogenic origin, *Journal of Geophysical Research*, vol. 112, D23S04, doi:10.1029/2006JD008094.

J. Genberg, M. Hyder, K. Stenström, R. Bergström, D. Simpson, E. O. Fors, J. Jönsson, E. Swietlicki, (2011). Source apportionment of carbonaceous aerosol in southern Sweden, *Atmos. Chem. Phys.*, 11, 11387–11400, doi:10.5194/acp-11-11387-2011.

Gongriep, F., (2011). Characterization of a system for the separation of the organic and elemental carbon content of aerosols, Bachelor Thesis at the University of Utrecht.

M.P. Keuken, M. Moerman, M. Voogt, M. Blom, E.P. Weijers, T. Röckmann, U. Dusek, (2013). Source contributions to PM_{2.5} and PM₁₀ at an urban background and a street location, *Atmospheric Environment* 71, p 26-35, <http://dx.doi.org/10.1016/j.atmosenv.2013.01.032>.

I. Levin, T. Naegler¹, B. Kromer, M. Diehl, R.J. Francey, A.J. Gomez-Pelaez, L.P. STEELE, D. Wagenbach, R. Weller, (2009). Observations and modelling of the global distribution and long-term trend of atmospheric ¹⁴CO₂, *Tellus* 62B, 26–46.

Monaco, M., (2011). The Contribution of Fossil Fuel to Organic and Elemental Carbon using ¹⁴C measurements at a rural site in the Netherlands, Master Thesis at the University of Utrecht.

D. Mooibroek, M. Schaap, E.P. Weijers, R. Hoogerbrugge, (2011). Source apportionment and spatial variability of PM_{2.5} using measurements at five sites in the Netherlands, *Atmospheric Environment* 45, p 4180-4191, doi:10.1016/j.atmosenv.2011.05.017.

U. Pöschl, (2011). Atmospheric Aerosols: Composition, Transformation, Climate and Health Effects, *Angew. Chem. Int. Ed.*, 44, 7520 – 7540.

Röckmann, T., (2010). Atmospheric composition and chemical processes (ACCP) part 1: gas phase chemistry and atmospheric budgets, Master Course NS-MO405M at the University of Utrecht.

Roelofs, G.J., (2010). Atmospheric composition and chemical processes, aerosol, clouds and radiation, Master Course NS-MO405M at the University of Utrecht.

S. Szidat, T.M. Jenk, H.W. Gäggeler, H.-A. Synal, I. Hajdas, G. Bonani, M. Saurer, (2004). THEODORE, a two-step heating system for the EC/OC determination of radiocarbon (¹⁴C) in the environment, *Nuclear Instruments and Methods in Physics Research B* 223–224, 829–836.

S. Szidat, M. Ruff, N. Perron, L. Wacker, H.-A. Synal, M. Hallquist, A. S. Shannigrahi, K. E. Yttri, C. Dye, D. Simpson, (2009). Fossil and non-fossil sources of organic carbon (OC) and elemental carbon (EC) in Göteborg, Sweden, *Atmos. Chem. Phys.*, 9, 1521–1535.

S. Szidat, A.S.H. Prévôt, J. Sandradewi, M. Rami Alfarra, H.A. Synal, Lukas Wacker, U. Baltensperger, (2007). Dominant impact of residential wood burning on particulate matter in Alpine valleys during winter, *Geophysical Research Letters*, VOL. 34, L05820, doi:10.1029/2006GL028325.

Szidat, S., Jenk, T.M., Synal, H.A., Kalberer, M., Wacker, L., Hajdas, I., Kasper-Giebl, A., Baltensperger, U., (2006). Contributions of fossil fuel, biomass-burning, and biogenic emissions to carbonaceous aerosols in Zurich as traced by ¹⁴C, *Journal of Geophysical Research*, vol. 111, D07206, doi:10.1029/2005JD006590.

K. E. Yttri, D. Simpson, K. Stenström, H. Puxbaum, T. Svendby, (2011). Source apportionment of the carbonaceous aerosol in Norway, quantitative estimates based on ¹⁴C, thermal-optical and organic tracer analysis, *Atmos. Chem. Phys.*, 11, 9375–9394.

Y. L. Zhang, N. Perron, V. G. Ciobanu, P. Zotter, M. C. Minguillón, L. Wacker, A. S. H. Prévôt, U. Baltensperger, S. Szidat, (2012). On the isolation of OC and EC and the optimal strategy of radiocarbon-based source apportionment of carbonaceous aerosols, *Atmos. Chem. Phys.*, 12, 10841–10856.

Websites;

http://ready.arl.noaa.gov/HYSPLIT_traj.php

IPCC report 2007;

http://www.ipcc.ch/publications_and_data/publications_and_data_reports.shtml#UmJPzmDxu00

<http://www.cesar-observatory.nl/index.php?pageID=7001>

<http://weather.uwyo.edu/upperair/sounding.html>

<http://www.wikipedia.org/>

7. Appendixes

Appendix A: THEODORE

THEODORE stands for “Two-step Heating system for the EC/OC Determination Of Radiocarbon in the Environment”.

Procedure THEODORE OC, TC and blanks, standards

At the beginning of the day:

- clean scissors and tweezers
- get liquid N₂
- check if the valve on the pressure flask is open
- if the helium and oxygen are ready to use: are valves near the ceiling open? (if not: open valves and flush system first with O₂, then with He for a bit)
- open valve on O₂ line, upstream of flow controller further inside the system
- Is the P₂O₅ in the water trap still ok? If moist and dirty, replace by new one, see (12)
- if there are enough breakseals/ storage flasks connected to the system If not, see (12)
- take filter holder out of oven
- if the reaction tube has been evacuated overnight (low pressure in reaction tube)
 - o check for leak by closing 3-way valve S, pressure in reaction tube should be stable
 - o keep valve S closed
 - o and fill the system with He (by switching gas valve G to He flow).
 - o When pressure in reaction tube is higher than ambient, close gas valve G.
 - o After that it is possible to open the reaction tube for introducing the sample (step 2)
- if the **temperature of the ovens** is set at the right value
 - o OC Oven 1 = 340, Oven 2 = 450, oven 3 = 650
 - o TC and standards: Oven 1 = 340, Oven 2 = 650, oven 3 = 650
- **Turn on Cu** oven
- **Prepare dry ice ethanol mixture**

1 PLACE FILTER IN SAMPLE HOLDER IN THE REACTION TUBE:

- o Close valve S and then G, if open
- o Put in filter (write **Pambient**)
- o close the tube

2 FLUSH THE SYSTEM WITH HELIUM:

- start helium flow with black valve (helium flow has no mass flow controller, but its flow is such that pressure in the reaction tube is 1050-1100 mb)
- Switch three-way valve S to the pump
- start timer
- Wait 10 min, if necessary get liquid N₂
- Write **PHe**

3 START O₂ FLOW:

- Switch gas valve to O₂, start flow controller
- Cool trap with liquid nitrogen
- Wait 5 min

4 BURN OC:

- Close HV + Close V2 red (trap2)
- Switch 3-way valve S to glass line
- Open LV pump
- take timer
- move sample to first oven for the corresponding time, depending on the type of extraction
- Use big black **X** on the table for the right sample position (for EC, blanks and standards: **I**)
- **Put dry-ice ethanol trap.**

5 CHECKS:

- Check pressure in reaction tube (should be below 1250 mbar) and glass line
- Check the flow of the mass flow controller (should be around 62 units on the mass flow controller)
- Write values (read after 10 min) in the lab book (**PO₂, O₂ flow, P glass line**).

6 FLUSH REACTION TUBE:

- When the extraction time is finished, switch three-way valve S to pump
- Leave at O₂ flow for a while (~10 min to clean system)
- Later switch to He flow and switch off O₂ flow controller with the little back switch

7 EVACUATE SYSTEM:

- Evacuate sample glass line with LV to below 30mbar
- Close LV
- Then turn on HV until pressure close to 0
- Open V2 on trap 2 and wait again until pressure close to 0
- Cool trap2

8 REMOVE NOX

- Close HV (after pressure close to 0)
- Turn T2 to Cu oven
- Turn T1 to He
- Take off liquid nitrogen trap1
- Heat trap1
- Wait 10 min, when pressure in the glass is > ambient open cap (put the glass cap with the hole)
- Write **PHe** trap2, then wait 10 min
- (Clean reaction tube with hot filter holder, then switch to He flow)
- After 10 min, close cap
- Close T1
- Evacuate with LV+HV
- Close V1 on trap2

9 REMOVE H₂O:

- **Close HV**
- Take away liquid nitrogen from trap2 and heat this with heat gun
- Observe pressure sensor. Pressure will increase and stabilize
- Cool the very bottom of the P2O5 vial with liquid Nitrogen
- Once pressure does not decrease anymore (check by closing off CO2 trap V2 for a short while, then open again), Raise liquid N2 on P2O5 vial, pump away rest of gases with HV
- Close P2O5 vial, remove liquid N2, and wait for 3 minutes
- Close valve V2 on CO2 trap.

10 DETERMINE CO₂ PRESSURE:

(If you expect lots of material it might be good to check pressure in the entire glass line before freezing the CO2 into pressure flask. If pressure in the glass line is below 20 mbar it's ok).

- **Close HV**
- Freeze CO2 into flask with pressure sensor. Start cooling at the bottom
- Once pressure does not decrease any more, pump away excess material
- close the pressure flask
- Remove liquid Nitrogen from pressure flask and bring flask to room temperature
- Read pressure once it stops changing (**POC, PEC, PTC**)

11 FREEZE TO BREAKSEAL OR OTHER FLASK:

- **Close HV**
- Open pressure vial
- freeze to new flask
- pump away excess material
- close flask or breakseal
- Remove liquid N2
- Write **Pzero**

12 REMOVE SAMPLES:

- **Close HV!!**

- Fill the glass line with He (read valve on sample glass line). Open slowly and close immediately again
- Remove flask or breakseals and replace with new ones
- Open new flasks
- Open LV, at pressure smaller 30mbar close LV, then open HV.

13 ENDING THE EXPERIMENT FOR ONE SAMPLE:

- open V1 and V2 on trap2
- **Close HV**
- Turn T2 to GL, T1 to RT
- Evacuate HV
- Start with next sample at point 1

13A ENDING THE LAST EXPERIMENT FOR THE DAY

- Turn off Cu oven.
- **Close HV**
- Open valves V1, V2 both traps
- Turn T1 to RT
- Turn T2 to GL
- Evacuate HV
- Remove **dry-ice/ethanol trap** and heat with the gun
- Close He flow (black valve G)
- Evacuate the whole system: switch 3-way valve S to sample glass line.
- Turn off O₂ black valve upstream of flow controller, further inside the system

Procedure THEODORE WIOC/EC

At the beginning of the day:

- clean scissors and tweezers
- get liquid N₂
- check if the valve on the pressure flask is open
- if the helium and oxygen are ready to use: are valves near the ceiling open? (if not: open valves and flush system first with O₂, then with He for a bit)
- open valve on O₂ line, upstream of flow controller further inside the system
- Is the P₂O₅ in the water trap still ok? If moist and dirty, replace by new one, see (12)
- if there are enough breakseals/ storage flasks connected to the system If not, see (12)
- take filter holder out of oven
- if the reaction tube has been evacuated overnight (low pressure in reaction tube)
 - o check for leak by closing 3-way valve S, pressure in reaction tube should be stable
 - o keep valve S closed
 - o and fill the system with He (by switching gas valve G to He flow).
 - o When pressure in reaction tube is higher than ambient, close gas valve G.
 - o After that it is possible to open the reaction tube for introducing the sample (step 1)
- if the **temperature of the ovens** is set at the right value
 - o Oven 1 = 370, Oven 2 = 450, oven 3 = 650
- **Turn on Cu oven**

1 PLACE FILTER IN SAMPLE HOLDER IN THE REACTION TUBE:

- o Close valve S and then G, if open
- o Put in filter (write **Pambient**)
- o close the tube

2 FLUSH THE SYSTEM WITH HELIUM:

- o start helium flow with black valve G (helium flow has no mass flow controller, but is flow is such that pressure in the reaction tube is 1050-1100 mb)
- o Switch three-way valve S to the pump
- o start timer
- o Wait 10 min, if necessary get liquid N₂
- o Write **PHe**

3 START O₂ FLOW:

- o Switch gas valve to O₂, start flow controller
- o Cool trap 1 with liquid nitrogen
- o Wait 5 min

4 BURN OC:

- o Close HV + Close V2 red (trap2)
- o Switch 3-way valve S to glass line

- Open LV pump
- take timer
- move sample to first oven for 15 min
- Use big black **X** on the table for the right sample position
- **Put dry-ice ethanol trap.**

5 CHECKS:

- Check pressure in reaction tube (should be below 1250 mbar) and glass line: 10-16 mbar
- Check the flow of the mass flow controller (should be around 50-60 units on the mass flow controller)
- Write values (read after 10 min) in the lab book (**PO₂, O₂ flow, P glass line**).

6 BURN REMAINING WIOC:

- When the extraction time is finished, switch three-way valve S to pump
- Set timer to two minutes
- Move filter to oven 2, start timer
- After 2 minutes, take filter out of ovens
- Set T oven 2 to 650 C

7 EVACUATE GLASS LINE:

- Close LV
- Then turn on HV until pressure close to 0
- Open V2 on trap 2 and wait again until pressure close to 0
- Cool trap2

8 REMOVE NOX

- Close HV (after pressure close to 0)
- Turn T2 to Cu oven
- Turn T1 to He
- Take off liquid nitrogen trap1
- Heat trap1
- Wait 5 min, when pressure in the glass is > ambient open cap (put the glass cap with the hole)
- Write **PHe** trap2, then wait 5 min
- (Clean reaction tube with hot filter holder, then switch to He flow)
- After 10 min, close cap
- Close T1
- Evacuate with LV+HV (12 min)
- Close V1 on trap2
- If last sample of the day, turn off Cu oven

9 REMOVE H₂O:

- **Close HV**
- Take away liquid nitrogen from trap2 and heat this with heat gun
- Observe pressure sensor. Pressure will increase and stabilize
- Cool the very bottom of the P2O5 vial with liquid Nitrogen

- Once pressure does not decrease anymore (check by closing off CO2 trap V2 for a short while, then open again), Raise liquid N2 on P2O5 vial, pump away rest of gases with HV
- Close P2O5 vial, remove liquid N2, and wait for 3 minutes
- Close valve V2 on CO2 trap.

10 DETERMINE CO₂ PRESSURE: (If you expect lots of material it might be good to check pressure in the entire glass line before freezing the CO2 into pressure flask. If pressure in the glass line is below 20 mbar it's ok).

- **Close HV**
- Freeze CO2 into flask with pressure sensor. Start cooling at the bottom
- Once pressure does not decrease any more, pump away excess material
- close the pressure flask
- Remove liquid Nitrogen from pressure flask and bring flask to room temperature
- Read pressure once it stops changing (**POC, PEC, PTC**)

11 FREEZE TO BREAKSEAL OR OTHER FLASK:

- **Close HV**
- Open pressure vial
- freeze to new flask
- pump away excess material
- close flask or breakseal
- Remove liquid N2
- Write **Pzero**

12 ENDING THE EXPERIMENT FOR WIOC SAMPLE:

- open V1 and V2 on trap2
- Turn T2 to GL, T1 to RT
- Evacuate HV
- Start with next sample at point 1

13 PREPARE FOR EC EXTRACTION:

- Cool trap 1 with liquid nitrogen
- Wait 5 min

14 BURN OC:

- Close HV + Close V2 red (trap2)
- Switch 3-way valve S to glass line
- Open LV pump
- take timer
- move sample to second oven for 15 min
- Use big black **I** on the table for the right sample position
- **Put dry-ice in ethanol trap.**

15 CHECKS:

- Check pressure in reaction tube (should be below 1250 mbar) and glass line
- Check the flow of the mass flow controller (should be around 62 units on the mass flow controller)
- Write values (read after 10 min) in the lab book (**P**O₂, **O**₂ flow, **P** glass line).

16 EXTRACT EC:

- When the extraction time is finished, switch three-way valve S to pump

17 EVACUATE GLASS LINE:

- Close LV when pressure < 20 mbar
- Then turn on HV until pressure close to 0

18 REMOVE H₂O:

- **Close HV**
- Close valve V1 on trap 1 (green)
- Take away liquid nitrogen from trap1 and heat this with heat gun
- Observe pressure sensor. Pressure will increase and stabilize
- Cool the very bottom of the P₂O₅ vial with liquid Nitrogen
- Once pressure does not decrease anymore (check by closing off CO₂ trap V2 for a short while, then open again), Raise liquid N₂ on P₂O₅ vial, pump away rest of gases with HV
- Close P₂O₅ vial, remove liquid N₂, warm up, and wait for 5 minutes
- Close valve V2 on CO₂ trap.

19 DETERMINE CO₂ PRESSURE:

(If you expect lots of material it might be good to check pressure in the entire glass line before freezing the CO₂ into pressure flask. If pressure in the glass line is below 20 mbar it's ok).

- **Close HV**
- Freeze CO₂ into flask with pressure sensor. Start cooling at the bottom
- Once pressure does not decrease any more, pump away excess material
- close the pressure flask
- Remove liquid Nitrogen from pressure flask and bring flask to room temperature
- Read pressure once it stops changing (**PEC**)
-

20 CLEAN REACTION TUBE

- Move hot filter holder in reaction tube
- Switch reaction tube to He flow
- Turn oven 2 to 450 C

21 FREEZE TO BREAKSEAL OR OTHER FLASK:

- **Close HV**
- Open pressure vial

- freeze to new flask
- pump away excess material
- close flask or breakseal
- Remove liquid N₂
- Write **Pzero**

22 REMOVE SAMPLES:

- **Close HV!!**
- Fill the glass line with He (read valve on sample glass line). Open slowly and close immediately again
- Remove flask or breakseals and replace with new ones
- Open new flasks
- Open LV, at pressure smaller 30mbar close LV, then open HV.

23A ENDING THE EXPERIMENT FOR EC SAMPLE:

- open V1 and V2 on trap2 and V1, V2 on trap 1
- Turn T2 to GL, T1 to RT
- Evacuate HV
- Start with next sample at point 1
- Take filter holder out of oven

23B ENDING THE LAST EXPERIMENT FOR THE DAY

- Turn off Cu oven.
- **Close HV**
- Open valves V1, V2 both traps
- Turn T1 to RT
- Turn T2 to GL
- Evacuate HV
- Remove **dry-ice/ethanol trap**
- Close He flow (black valve G)
- Evacuate the whole system: switch 3-way valve S to sample glass line.
- Turn off O₂ black valve upstream of flow controller, further inside the system

Procedure removing WIOC and OC

At the beginning of the day:

- clean scissors and tweezers
- get liquid N₂
- check if the valve on the pressure flask is open
- if the helium and oxygen are ready to use: are valves near the ceiling open? (if not: open valves and flush system first with O₂, then with He for a bit)
- open valve on O₂ line, upstream of flow controller further inside the system
- Is the P₂O₅ in the water trap still ok? If moist and dirty, replace by new one, see (12)
- if there are enough breakseals/ storage flasks connected to the system If not, see (12)
- take filter holder out of oven
- if the reaction tube has been evacuated overnight (low pressure in reaction tube)
 - o check for leak by closing 3-way valve S, pressure in reaction tube should be stable
 - o keep valve S closed
 - o and fill the system with He (by switching gas valve G to He flow).
 - o When pressure in reaction tube is higher than ambient, close gas valve G.
 - o After that it is possible to open the reaction tube for introducing the sample (step 1)
- if the **temperature of the ovens** is set at the right value
 - o Oven 1 = 370, Oven 2 = 450, oven 3 = 650
- **Turn on Cu oven**

1 PLACE FILTER IN SAMPLE HOLDER IN THE REACTION TUBE:

- o Close valve S and then G, if open
- o Put in filter (write **Pambient**)
- o close the tube

2 FLUSH THE SYSTEM WITH HELIUM:

- o start helium flow with black valve G (helium flow has no mass flow controller, but the flow is such that pressure in the reaction tube is 1050-1100 mb)
- o Switch three-way valve S to the pump
- o start timer
- o Wait 10 min, if necessary get liquid N₂
- o Write **PHe**

3 START O₂ FLOW:

- o Switch gas valve to O₂, start flow controller

4 BURN OC:

- o take timer
- o move sample to first oven for 15 min
- o Use big black **X** on the table for the right sample position

5 CHECKS:

- Check pressure in reaction tube (should be below 1250 mbar)
- Check the flow of the mass flow controller (should be around 50-60 units on the mass flow controller)
- Write values (read after 10 min) in the lab book (**PO₂**, **O₂ flow**).

6 BURN REMAINING WIOC:

- Set timer to two minutes
- Move filter to oven 2, start timer
- After 2 minutes, take filter out of ovens

7 ENDING THE EXPERIMENT FOR REMOVING WIOC:

- start helium flow with black valve G (helium flow has no mass flow controller, but the flow is such that pressure in the reaction tube is 1050-1100 mb)
- Stop O₂ flow controller
- Close valve S and then G.
- Take filter holder out of oven
- Put filter in aluminium foil
- Start with next sample at point 1

8 CLEAN REACTION TUBE

- Move hot filter holder in reaction tube
- Switch reaction tube to He flow
- Turn oven 2 to 450 C

9 ENDING THE LAST EXPERIMENT FOR THE DAY

- Turn off Cu oven, if it was still on of course.
- **Close HV**
- Open valves V1, V2 both trap, if closed
- Turn T1 to RT
- Turn T2 to GL
- Evacuate HV
- Remove **dry-ice/ethanol trap**, if it was still there.
- Close He flow (black valve G)
- Evacuate the whole system: switch 3-way valve S to sample glass line.
- Turn off O₂ black valve upstream of flow controller, further inside the system

